A Mechanoresponsive Heterochiral Hydrogelator as a potential Matrix Metalloproteinase 2 Inhibitor : Unravelling its Anti-inflammatory Efficacy in vitro and in vivo

Anita Dutt Konar [a, b,c],* Vaibhav Shivhare,[a] Rishabh Ahuja,[a] Priyanka Tiwari,[a] Naureen Khan,[a] Surendra Kumar Ahirwar, [a] Avinash Singh Mandloi,[c] Ankit Mishra,[c] Anindya Basu [b,c]

Table of Contents

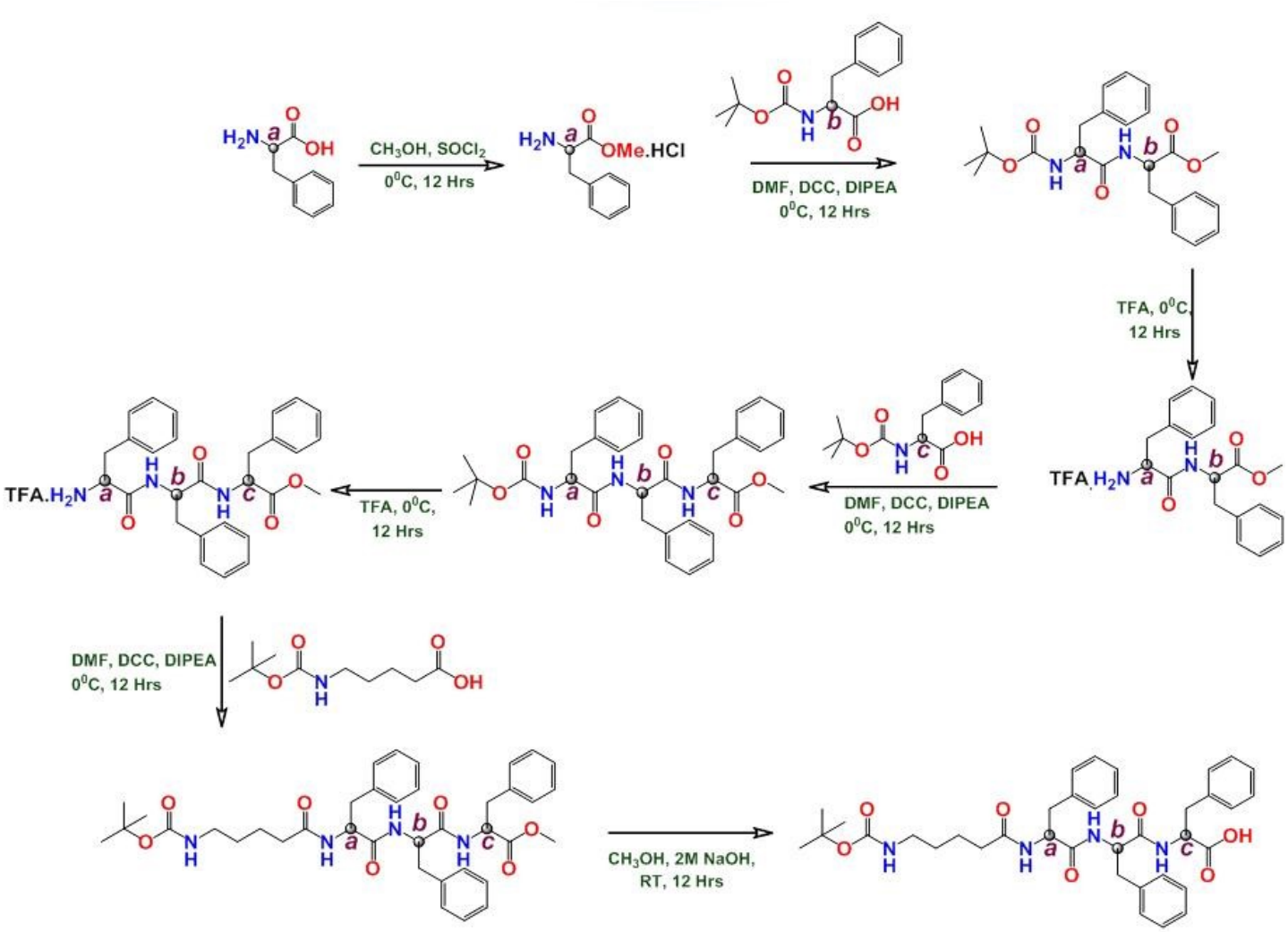

	a)	b)	c)
Hydrogelator **I**	**L**	**L**	**L**
Hydrogelator **II**	**L**	**L**	**D**
Hydrogelator **III**	**L**	**D**	**D**
Hydrogelator **IV**	**D**	**D**	**D**
Hydrogelator **V**	**D**	**D**	**L**
Hydrogelator **VI**	**L**	**D**	**L**
Hydrogelator **VII**	**D**	**L**	**D**
Hydrogelator **VIII**	**D**	**L**	**L**

Figure S-1: - Synthesis Scheme for Hydrogelators **I - VIII**

Experimental Techniques Adopted

Synthesis of the Hydrogelators: Conventional solution phase methodology was employed in order to synthesize the hydrogelators with racemization free techniques as described in the Scheme as follow. Thin Layer Chromatography (TLC) on silica gel was used to check the purity of the obtained intermediates. The final products were purified through column chromatography by silica gel (100-200 mesh) as the stationary phase and the mixture of ethyl acetate and petroleum ether as the eluent.

Synthesis of the dipeptides: Boc-(Y)-Phe-(Z)-Phe-OMe: The Y-Phe-OMe obtained from its hydrochloride (4.07 gm, 18.93 mmol) was added to an ice cold solution of Boc-X-Phe-OH (2 gm, 7.54 mmol) in 15 ml of DMF. Then DCC (2.33 gm, 11.31 mmol: 1, 3-dicyclohexylcarbodiimide) was added to the cooled mixture, which was stirred for 18 hours in ice cold condition. The progress of the reaction was monitored by TLC. The residue was taken into ethyl acetate and the DCU was filtered off. The organic layer was washed with 2 M HCl (3 × 100), 1 M Sodium carbonate (3 × 100 ml) and brine (2 × 100 ml), dried over anhydrous sodium sulphate and evaporated in *vacuum* to obtain a white solid material. The crude peptide was used without further purification.

Yield: Y=L; Z=L: 2.43 g (5.70 mmol, 75 %)

Synthesis of Boc-(X)-Phe-(Y)-Phe-(Z)-Phe-OMe: To Boc-(X)-Phe-(Y)-Phe -OMe (the exact amount obtained from the above step) trifluoroacetic acid (10 ml, minimum amount) was added at 0^0C and the mixture was stirred at room temperature. The removal of the Boc group was monitored by TLC. After 12 h the trifluoroacetic acid was removed under reduced pressure to afford the crude trifluoroacetate salt. This dipeptide salt was treated with $NaHCO_3$ and extracted by ethyl acetate, and added to an ice cold solution of Boc-X-Phe-OH (1.51 gm, 5.70 mmol) in 15 ml of DMF. Then DCC (1.8 gm, 9.16 mmol: 1, 3-dicyclohexylcarbodiimide) was added to the cooled mixture, which was stirred for 18 hours in ice cold condition. The progress of the reaction was monitored by TLC. The residue was taken into ethyl acetate and the DCU was filtered off. The organic layer was washed with 2 M HCl (3 × 100), 1 M Sodium carbonate (3 × 100 ml) and brine (2 × 100 ml), dried over anhydrous sodium sulphate and evaporated in *vacuum* to obtain a white solid material. The crude peptide was used without further purification.

Yield: X=D; Y=Z=L 2.77 g (4.83 mmol, 85 %)

Synthesis of Boc-Ava-(X)-Phe-(Y)-Phe-(Z)-Phe-OMe: To Boc-(X)-Phe-(Y)-Phe-(Z)-Phe -OMe (the exact amount obtained from the above step) trifluoroacetic acid (12 ml, minimum amount) was added at 0^0C and the mixture was stirred at room temperature. The removal of the Boc group was monitored by TLC. After 12 h the trifluoroacetic acid was removed under reduced pressure to afford the crude trifluoroacetate salt. This dipeptide salt was treated with $NaHCO_3$ and extracted by ethyl acetate, and added to an ice cold solution of Boc-Ava-OH (1.05 gm, 4.83 mmol) in 10 ml of DMF. Then DCC (1.60

gm, 7.59 mmol: 1, 3- dicyclohexylcarbodiimide) was added to the cooled mixture, which was stirred for 18 hours in ice cold condition. The progress of the reaction was monitored by TLC. The residue was taken into ethyl acetate and the DCU was filtered off. The organic layer was washed with 2 M HCl (3 × 100), 1 M Sodium carbonate (3 × 100 ml) and brine (2 × 100 ml), dried over anhydrous sodium sulphate and evaporated in *vacuum* to obtain a white solid material. The crude peptide was used without further purification

Yield: Boc-Ava X=D; Y=Z=L: 2.42 g (4.83 mmol, 75 %)

Synthesis of Boc-Ava-(X)-Phe-(Y)-Phe-(Z)-Phe-OH: Boc-Ava-(X)-Phe-(Y)-Phe-(Z)-Phe-OMe was dissolved in calculated amount of methanol (20 ml) and NaOH (2M NaOH: 14 ml) was added dropwise to the solution. The progress of the reaction was monitored by TLC. After completion of the reaction, as determined by TLC, the methanol was evaporated. The residue containing the sodium salt was dissolved in water and extracted with diethyl ether to remove the unreacted stuff. The aqueous layer obtained was cooled, acidified with 2N HCl and extracted with ethyl acetate. The solvent was evaporated *in vacuo* to obtain a white solid.

Yield: Boc-Ava - X=D; Y=Z=L: 1.65 g (3.60 mmol, 70 %)

A) Hydrogelator-**I:(L-L-L):** Yield: 2.06 gm (80%); **LC-MS:** $C_{37}H_{46}N_4O_7$: 659.5 $[M + H]^+$; MS (calculated) m/z ; 658.5 $[M]^+$**;** **^{1}H NMR** (500 MHz; d_6-DMSO; δ in ppm):12.97 – 12.44 (-COOH Phe(3), 1H, br); 8.48 (Phe(3)NH, 1H, d, *J* = 10Hz); 8.24 (Phe(2)NH, 1H, d, *J* = 10Hz); 7.82 (Phe(1)NH, 1H, d, *J* = 10Hz); 7.29 – 7.16 (Phe(1), Phe(2) & Phe(3) aromatic Hs, 15H, m); 7.03 – 7.01 (Ava(1)NH, 1H, m); 4.53 – 4.41 (Phe(1), Phe(2) & Phe(3) $C^{\alpha}H$, 3H, m) ; 4.62 – 4.53 (Ava(1), $C^{\alpha}Hs$, 2H, m); 3.14 – 3.06 (Ava(1), $C^{\delta}Hs$, 2H, m); 2.93 – 2.77 (Phe(1), Phe(2) & Phe(3), $C^{\beta}Hs$, 6H, m); 2.40 – 2.35 (Ava(1), $C^{\beta}Hs$, 1H, m); 2.27 – 2.10 (Ava(1), $C^{\beta}Hs$, 1H, m); 1.37 (Boc-Mes, 9H, s); 1.19 – 1.14 (Ava(1), $C^{\gamma}H$, 1H, m).

B) Hydrogelator-**II:(L-L-D) :** Yield: 2.06 gm (80%); **LC-MS:** $C_{37}H_{46}N_4O_7$: 659.5 $[M + H]^+$; MS (calculated) m/z ; 658.5 $[M]^+$**;** **^{1}H NMR** (500 MHz; d_6-DMSO; δ in ppm):12.64 – 11.95 (-COOH Phe(3), 1H, br); 8.46 (Phe(3)NH, 1H, d, *J* = 10Hz); 8.25 (Phe(2)NH, 1H, d, *J* = 10Hz); 7.82 (Phe(1)NH, 1H, d, *J* = 10Hz); 7.27 – 7.18 (Phe(1), Phe(2) & Phe(3) aromatic Hs, 15H, m); 6.69 – 6.66 (Ava(1)NH, 1H, m); 4.46 – 4.42 (Phe(1), Phe(2) & Phe(3) $C^{\alpha}H$, 3H, m) ; 4.61 – 4.54 (Ava(1), $C^{\alpha}Hs$, 2H, m); 3.12 – 3.09 (Ava(1), $C^{\delta}Hs$, 2H, m); 2.83 – 2.76 (Phe(1), Phe(2) & Phe(3), $C^{\beta}Hs$, 6H, m); 2.39 – 2.37 (Ava(1), $C^{\beta}Hs$, 2H, m); 1.37 (Boc-Mes, 9H, s); 1.19 –1.16 (Ava(1), $C^{\gamma}H$, 1H, m).

C) Hydrogelator-**III:(L-D-D) :** Yield: 1.80 gm (70%); **LC-MS:** $C_{37}H_{46}N_4O_7$: 659.5 $[M + H]^+$; MS (calculated) m/z ; 658.5 $[M]^+$**;** **^{1}H NMR** (500 MHz; d_6-DMSO; δ in ppm):13.00 – 12.62 (-COOH Phe(3), 1H, br); 8.49 (Phe(3)NH, 1H, d, *J* = 10Hz); 8.24 (Phe(2)NH, 1H, d, *J* = 10Hz); 7.82

(Phe(1)NH, 1H, d, *J* = 10Hz); 7.29 – 7.16 (Phe(1), Phe(2) & Phe(3) aromatic Hs, 15H, m); 6.69 – 6.66 (Ava(1)NH, 1H, m); 4.51 – 4.33 (Phe(1), Phe(2) & Phe(3) $C^{\alpha}H$, 3H, m) ; 4.62 – 4.53 (Ava(1), $C^{\alpha}Hs$, 2H, m); 3.14 – 3.05 (Ava(1), $C^{\delta}Hs$, 2H, m); 2.91 – 2.77 (Phe(1), Phe(2) & Phe(3), $C^{\beta}Hs$, 6H, m); 2.40 – 2.35 (Ava(1), $C^{\beta}Hs$, 1H, m); 1.97 – 1.95 (Ava(1), $C^{\beta}Hs$, 1H, m); 1.38-1.37 (Boc-Mes, 9H, s); 1.18 – 1.17 (Ava(1), $C^{\gamma}H$, 1H, m).

D) Hydrogelator-**IV:(D-D-D) :** Yield: 1.93 gm (75%); **LC-MS:** $C_{37}H_{46}N_4O_7$: 659.5 $[M + H]^+$; MS (calculated) m/z ; 658.5 $[M]^+$**; ^{1}H NMR** (500 MHz; d_6-DMSO; δ in ppm):16.00 (-COOH Phe(3), 1H, br); 8.35 (Phe(3)NH, 1H, d, *J* = 10Hz); 8.28 (Phe(2)NH, 1H, d, *J* = 10Hz); 7.82 (Phe(1)NH, 1H, d, *J* = 10Hz); 7.27 – 7.14 (Phe(1), Phe(2) & Phe(3) aromatic Hs, 15H, m); 6.68 – 6.64 (Ava(1)NH, 1H, m); 4.47 – 4.44 (Phe(1), Phe(2) & Phe(3) $C^{\alpha}H$, 3H, m) ; 4.58 – 4.54 (Ava(1), $C^{\alpha}Hs$, 2H, m); 3.11 – 3.08 (Ava(1), $C^{\delta}Hs$, 2H, m); 2.82 – 2.76 (Phe(1), Phe(2) & Phe(3), $C^{\beta}Hs$, 6H, m); 2.41 – 2.34 (Ava(1), $C^{\beta}Hs$, 1H, m); 2.22 – 2.17 (Ava(1), $C^{\beta}Hs$, 1H, m); 1.36 (Boc-Mes, 9H, s); 1.30 –1.28 (Ava(1), $C^{\gamma}H$, 1H, m).

E) Hydrogelator-**V:(D-D-L) :** Yield: 1.67 gm (65%); **LC-MS:** $C_{37}H_{46}N_4O_7$: 659.5 $[M + H]^+$; MS (calculated) m/z ; 658.5 $[M]^+$**; ^{1}H NMR** (500 MHz; d_6-DMSO; δ in ppm):16.00 (-COOH Phe(3), 1H, br); 8.46 (Phe(3)NH, 1H, d, *J* = 10Hz); 8.21 (Phe(2)NH, 1H, d, *J* = 10Hz); 7.83 (Phe(1)NH, 1H, d, *J* = 10Hz); 7.27 – 7.17 (Phe(1), Phe(2) & Phe(3) aromatic Hs, 15H, m); 6.66 – 6.64 (Ava(1)NH, 1H, m); 4.47 – 4.44 (Phe(1), Phe(2) & Phe(3) $C^{\alpha}H$, 3H, m) ; 4.57 – 4.54 (Ava(1), $C^{\alpha}Hs$, 2H, m); 3.11 – 3.09 (Ava(1), $C^{\delta}Hs$, 2H, m); 2.83 – 2.78 (Phe(1), Phe(2) & Phe(3), $C^{\beta}Hs$, 6H, m); 2.39 – 2.37 (Ava(1), $C^{\beta}Hs$, 1H, m); 2.21 – 2.18 (Ava(1), $C^{\beta}Hs$, 1H, m); 1.36 (Boc-Mes, 9H, s); 1.29-1.28 (Ava(1), $C^{\gamma}H$, 1H, m).

F) Hydrogelator-**VI:(L-D-L):** Yield: 1.93 gm (75%); **LC-MS:** $C_{37}H_{46}N_4O_7$: 659.5 $[M + H]^+$; MS (calculated) m/z ; 658.5 $[M]^+$**; ^{1}H NMR** (500 MHz; d_6-DMSO; δ in ppm):13.30 – 12.42 (-COOH Phe(3), 1H, br); 8.49 (Phe(3)NH, 1H, d, *J* = 10Hz); 8.24 (Phe(2)NH, 1H, d, *J* = 10Hz); 7.82 (Phe(1)NH, 1H, d, *J* = 10Hz); 7.29 – 7.14 (Phe(1), Phe(2) & Phe(3) aromatic Hs, 15H, m); 6.69 – 6.66 (Ava(1)NH, 1H, m); 4.52 – 4.46 (Phe(1), Phe(2) & Phe(3) $C^{\alpha}H$, 3H, m) ; 4.62 – 4.56 (Ava(1), $C^{\alpha}Hs$, 2H, m); 3.14 – 3.07 (Ava(1), $C^{\delta}Hs$, 2H, m); 2.93 – 2.77 (Phe(1), Phe(2) & Phe(3), $C^{\beta}Hs$, 6H, m); 2.40 – 2.18 (Ava(1), $C^{\beta}Hs$, 1H, m); 2.14 – 1.92 (Ava(1), $C^{\beta}Hs$, 1H, m); 1.38 (Boc-Mes, 9H, s); 1.30 – 1.27 (Ava(1), $C^{\gamma}H$, 1H, m); 1.17 – 1.15 (Ava(1), $C^{\gamma}H$, 1H, m).

G) Hydrogelator-**VII:(D-L-D):** Yield: 1.80 gm (70%); **LC-MS:** $C_{37}H_{46}N_4O_7$: 659.5 $[M + H]^+$; MS (calculated) m/z ; 658.5 $[M]^+$**; ^{1}H NMR** (500 MHz; d_6-DMSO; δ in ppm):12.56 – 11.76 (-COOH Phe(3), 1H, br); 8.48 (Phe(3)NH, 1H, d, *J* = 10Hz); 8.24 (Phe(2)NH, 1H, d, *J* = 10Hz); 7.82 (Phe(1)NH, 1H, d, *J* = 10Hz); 7.28 – 7.16 (Phe(1), Phe(2) & Phe(3) aromatic Hs, 15H, m); 7.03 – 7.02 (Ava(1)NH, 1H, m); 4.51 – 4.44 (Phe(1), Phe(2) & Phe(3) $C^{\alpha}H$, 3H, m) ; 4.61 – 4.54 (Ava(1), $C^{\alpha}Hs$, 2H, m); 3.12 – 3.10 (Ava(1), $C^{\delta}Hs$, 2H, m); 2.91 – 2.89 (Phe(1), Phe(2) & Phe(3), $C^{\beta}Hs$, 6H, m); 2.39

– 2.36 (Ava(1), $C^{\beta}Hs$, 1H, m); 2.14 – 2.10 (Ava(1), $C^{\beta}Hs$, 1H, m); 1.38-1.37 (Boc-Mes, 9H, s); 1.18 – 1.16 (Ava(1), $C^{\gamma}H$, 1H, m).

Yield:

Hydrogelator-**VIII:(D-L-L) : Yield: 1.65 gm (70%); LC-MS:** $C_{37}H_{46}N_4O_7$: 659.5 $[M + H]^+$; MS (calculated) m/z ; 658.5 $[M]^+$**; ^{1}H NMR** (500 MHz; d_6-DMSO; δ in ppm):12.98 – 12.58 (-COOH Phe(3), 1H, br); 8.50 (Phe(3)NH, 1H, d, *J* = 10Hz); 8.34 (Phe(2)NH, 1H, d, *J* = 10Hz); 8.23 (Phe(1)NH, 1H, d, *J* = 10Hz); 7.29 – 7.17 (Phe(1), Phe(2) & Phe(3) aromatic Hs, 15H, m); 6.67 – 6.64 (Ava(1)NH, 1H, m); 4.62 – 4.44 (Phe(1), Phe(2) & Phe(3) $C^{\alpha}H$, 3H, m) ; 4.18 – 4.00 (Ava(1), $C^{\alpha}Hs$, 2H, m); 3.14 – 3.05 (Ava(1), $C^{\delta}Hs$, 2H, m); 3.05 – 2.67 (Phe(1), Phe(2) & Phe(3), $C^{\beta}Hs$, 6H, m); 2.23 – 2.18 (Ava(1), $C^{\beta}Hs$, 1H, m); 1.51 – 1.43 (Ava(1), $C^{\beta}Hs$, 1H, m); 1.28-1.26 (Boc-Mes, 9H, s); 1.16 – 1.11 (Ava(1), $C^{\gamma}H$, 1H, m); **^{13}C NMR** (125 MHz; d_6-DMSO; δ in ppm)**:** 174.87, 173.23, 173.20, 172.24, 171.73, 171.46, 171.33, 155.98, 137.95, 137.82, 129.73, 129.60, 128.71, 128.37, 126.92, 126.69, 126.49, 79.64, 77.75, 53.95, 38.71, 38.24, 37.11, 35.25, 33.76, 29.32, 28.74, 22.89, 22.29: **FTIR :** 3528 cm^{-1}, 3468 cm^{-1}, 3002 cm^{-1}, 1640 cm^{-1}, 1524 cm^{-1}, 1368 cm^{-1} and 1178 cm^{-1}.

DFT Calculations

The molecules were created using Spartan08 software package and structure optimizations were done using a molecule of hydrogelator in Gaussian09.[1,2] B3LYP method was used along with 6-31G basis set. Optimization and frequency calculations were done using tight convergence criteria and all the negative frequencies were removed to get the structure at it's minimum potential energy. Partition coefficients were calculated by optimizing the structures in water and n-octanol as solvent using CPCM model in Gaussian09. The solvation energies obtained from minimizations with all positive frequencies were considered. The partition coefficient was calculated using the formula:

$$\log P = \frac{-\Delta G_{n-octanol/water}}{RTln10} \qquad \text{where, } \Delta G^{\circ}_{\text{n-octanol/water}} = \Delta G^{\circ}_{\text{n-octanol}} - \Delta G^{\circ}_{\text{water}}$$

Hydrogel Preparation

A required amount of Hydrogelator **VIII** was separately dissolved in 7.5 pH phosphate buffer and gently warmed until a clear solution was formed. It was left undisturbed for some time until the solvent was immobilized, and the formation of gels was confirmed by the inverted test tube method.

Anti-inflammatory Activities *in vitro*

Preparation of MMP samples: The tissue samples were minced completely with 5ml of tris buffer, centrifuged for 15 min at 3000rpm, and refrigerated for further use.

Preparation of extract: 50 µl of MMP sample along with 50 µl of the hydrogel was incubated for an hour. Only the MMPs were used as negative control (NC) and MMPs with 50 µl of Tetracycline

Hydrochloride (incubated for 1hr) were used as positive control. The solutions were mixed with 2x non reducing buffer in equal volume and 20 µl of sample was loaded in each well, the electrodes were connected and power was started. It was run at about 50V for 15 min and then 100V until the bromophenol blue reached the bottom of the plates. After electrophoresis, the apparatus was dissembled, the gel was removed and washed with zymogram renaturing buffer i.e.2.5%Triton x-100 for one hour to remove SDS completely allowing the gels to denature. It was further incubated at 37ºC overnight. Staining was done with Coomassie blue R-250 for one hour and then destained with appropriate solution. After staining, the background stains blue with Coomassie stain where the gelatin is degraded white bands appear indicating the presence of gelatinases. The lower bands are gelatinases-A(MMP-2) which is about 72KD while the upper bands are gelatinases-B(MMP-9) which runs at about 95KD. The percentage inhibition of protein denaturation was calculated by using the following formula % Inhibition = 100 x (Abs of control -Abs of sample) /Abs of control.

Docking studies

The atomic coordinates of MMP2 in complexation with Ar-yloxy phenylcarboxamide-heptapeptide (heptapeptide: Glu-Asp-Gln-Leu-NMe-Glu-Pro) as co-crystallized ligand (PDB ID: 7XJO) with resolution of 2Å was downloaded from the Pro-tein Data Bank. The structures were imported into the Maes-tro module (v9.3) available in the Schrödinger Trial package and the protein was optimized using the Protein Preparation Wizard. The other detailed procedures were followed using ref.

Antimicrobial Experiment of Hydrogelator VIII

***Bacterial Culture*:** The microorganisms were obtained as lyophilized powder were obtained from NCCS, Pune. Fresh inoculums of the organisms were prepared before commencing the experiments.

Optical density methods were employed in order to study the *in vitro* antimicrobial activity of all the hydrogelators against the reported organisms as described in the reference. (*New J. Chem*. 2020, **44**, 6346-6354). A series of 10 dilutions were used. Ten microliter of peptide hydrogels of concentrations 100 µg/ml was added to each well in triplicate (final concentrations were reported in the figures after dilutions), which was further diluted for rest of the experiments. Here, bacterial solution excluding the nutrient broth was used as a control while only the nutrient broth was used as a blank. Plates consisting of test organisms and hydrogels were incubated at 37 ºC for 24 hours. Microplate reader (Synergy H1 multimode microplate reader using 96-well microplates at 25 °C) was used to confirm the antibacterial behaviour of the peptide hydrogels by comparing the absorbance of the test solution and control experiment.

Proteolytic and Biocompatibility Studies of Hydrogelator VIII

To examine the proteolytic stability, Hydrogelators **VIII** was incubated with the proteolytic enzyme proteinase K for 48 h and the degradation recording by mass spectrometry at regular intervals of time of 12 h.

MTT Viability Assay

The cells were put into 96-well plates overnight at 37°C in 95% humidity and 5% CO_2. Hydrogelators of different concentrations were studied (15.78, 31.25, 62.5, 125, 250 and 500 μg/mL) and incubated for another 48 hours. After washing with the PBS buffer twice, 20 μL of the MTT solution was added to each well plate and incubation was done at 37°C. In order to dissolve the formazan crystals, 100 μL dimethyl sulfoxide (DMSO) was added to each well after 4 hours and absorbance was noted at 570 nm using a microplate reader.

Hemolytic Assay.

Blood Collection: This was done by collecting fresh whole blood (5 mL) from healthy male human volunteers devoid of any oral contraceptive, anticoagulant therapy or anti inflammatory therapy. The blood was centrifuged for 10 mins at 3000 rpm, washed with equal amount of normal saline. The process was repeated twice. RBCs were kept in a test tube with an anticoagulant EDTA under standard conditions of temperature 23±2 °C and relative humidity 55±10%.

Hemolysis Assay: Aliquots (5 ml) of the isotonic buffer, containing different concentration (6.25, 12.5, 25, 50, 100 and 200 μg/ml) of samples were treated in duplicate. PBS was used as a blank, whereas control samples were having erythrocytes in buffer and were devoid of treated samples. To each tube, erythrocyte suspension (30 μL) was added mixed gently by inversion. For 1 hour, the mixtures were then incubated at 37 °C. Thereafter, as the incubation was completed , the mixtures were centrifuged at 1000 rpm for 10 min at 4°C. Supernatant was collected in separate tube and absorbance was recorded with a 550 nm using micro plate reader. The % hemolysis was calculated as: H (%) = (O.D550 nm Sample –OD550 nm Negative Control) / (OD550nm positive Control– OD 550nm Negative Control)*100. Positive and negative controls induced 100% and 0% of lysis, respectively.

Lipid Peroxidation Assay. Isolated erythrocytes were washed thrice with PBS. Packed cell volume was adjusted to 5% with PBS, pH 7.4. In each tube, 990 μL of the cell suspension along with 10 μL of initial hydrogel concentrations (ranging from 20 to 0.312 mM) was used. In control tubes, 10 μL of buffer was added to the cell suspension, whereas only PBS without any cell was used as a blank. Each group was assigned six tubes (N = 6). Samples were then incubated for 1 h at 37 °C, followed by the addition of 2 mL of 28% trichloroacetic acid solution. Then, samples were centrifuged at 1000 rpm for 5 min and 2 mL of supernatant was collected from each tube. In each tube, 500 μL of 1%

thiobarbituric acid was added and samples were placed on a boiling water bath for 1 h followed by cooling under running tap water. Samples were centrifuged again for 5 min at room temperature at 5000 rpm, and absorbance was taken at 532 nm against blank. Simultaneously, a standard curve was made for malondialdehyde (MDA), ranging from 0.1 to 10 nM/mL prepared in 10 mM PBS by following the same procedure as mentioned above. The standard curve was used to calculate the amount of thiobarbituric acid-reactive substances (TBARs) formed equivalent to MDA formed in nanomolemilliliter (nM/mL). Similarly, top five higher concentrations (1.5, 2.5, 5, 10, and 20 mM) of both the hydrogels were also evaluated for lipid peroxidation (LPO) study. The erythrocytes were directly mixed in hydrogels (20 mM) and incubated for 1 h for the LPO experiment.

Determination of Conformation of Hydrogelator VIII.

The temperature dependent ^{1}H, NMR experiments were performed using Bruker Advance instrument operating at 500MHz NMR, with d_6-DMSO as solvent.

Fourier-Transform Infrared (FTIR) Spectroscopy

FTIR spectra for all the xerogels were recorded using a KBr pellet on an Agilent CARY 620 FTIR spectrophotometer. The background was collected using a blank KBr pellet.

Circular Dichroism

Far-UV CD measurements of the Hydrogelators were recorded in methanol at 25^{o}C with a 0.5 s averaging time, a scan speed of 50nm/min, using a JASCO spectropolarimeter (J 720 model) equipped with a 0.1 cm path length cuvette. The measurements were taken at 0.2 nm wavelength intervals, 2.0 nm spectral bandwidth, and five sequential scans were recorded for each sample.

Morphological Study of the Hydrogels.

Field-emission scanning electron microscopy (FE-SEM) experiment was performed on a JEOL scanning electron microscope (model no. JSM-7600F) with xerogels, obtained from the hydrogels of same concentration 6 mg/ml.

Determination of Mechanical Strength of the Hydrogelators.

Anton PaarPhysica MCR 301 rheometer was employed at 25 °C to perform the Rheological Experiments. The viscoelastic properties of hydrogels were measured by measuring the storage modulus (G′) and loss modulus (G″). 1mL hydrogel was put on a rheometer plate with the help of a microspatula and was hydrated using a solvent trap. The hydrogels were sandwiched with TruGap (0.5 mm) using a stainless steel plate (diameter: 25 mm). To determine the region of deformation of hydrogels, dynamic strain sweep experiments were done in which viscoelasticity was valid. The exact strains for hydrogel materials were determined by linear viscoelastic regime at a constant frequency of 10 rad s^{-1}. In order to ascertain the mechanical strengths of the hydrogels, frequency sweep experiments were performed. During this, the graph was plotted as a function of frequency ranging from 0.05 to 100 rad s^{-1}. While step-strain experiments were

used to investigate the thixotropic behaviour of the hydrogels where the applied strain varied from 0.1 to 40%. The concentrations of hydrogelators used were 6 mg/mL.

Anti-inflammatory activities *in vivo*

In-vivo activity for anti-inflammatory potential was evaluated in Albino mice of either sex weighing 30±6gm. Prior approvals from animal ethical committee Faculty of Pharmacy VNS Group of Institutions, Bhopal CPCSEA REG.NO.778/PO/ReBi/S/03/CPCSEA 03/09/2012 meeting held in November 2023. Animals were taken from the animal house of the Faculty of Pharmacy VNS Group of Institutions, Bhopal, which maintained a 12-hour light-dark cycle, with temperature and humidity controlled as per standard. Standard food and drinking water were sufficiently available to the animals.

Experimental procedure: Animals were divided into four groups, each containing six animals: Control Group, disease-controlled group, standard group and high dose 1%w/v.

Except for the control group, a dorsal air sac was formed in all groups by injecting 4 ml of sterile air prepared subcutaneously by air filtration through a 0.2 µm Hi-media India syringe filter on the first day. On the 3rd day, 3 mL of sterile air was loaded to tighten the local tissues. On the fifth day, all groups except the control group were injected with 0.1 ml of 1% (w/v) carrageenan solution prepared with vigorous shaking and kept overnight to induce acute inflammation. On the same day, the fifth day, four hours after the injection of carrageenan, the standard drug Diclofenac sodium (Voveran® injection) was injected with a dose of 10 mg/kg of body weight. 0.1 ml of both a low dose of 0.5% w/v% and a high dose of 1% w/v. was injected. Blood samples were collected by retroorbital puncture on the seventh day and analyzed for hematological analysis. Animals were sacrificed by cervical dislocation, and inflammatory tissues were collected and evaluated for biochemistry and histology.

Protein Expression Analysis with ELISA – IL-6

Experiment was performed as per kit instructions (GENLISA™ Rat Interleukin 6 (IL-6) ELISA- Cat No.: KLR0135 kit) 100 μl standard (IL- 6 - 1 µg/ml) and sample was added to the plate, plate was sealed and incubated for 2 h at room temperature. Plate was washed four times with wash buffer (1X) and buffer was blotted by firmly tapping plate upside down on absorbent paper. Diluted detection antibody (Biotin Conjugated Detection Antibody) solution was added 100µl to each well, plate was sealed and incubated for an hour at room temperature. Again, plate was washed with wash buffer (1X) then 100µl diluted Streptavidin -HRP solution was added to each well, plate was sealed and incubated for an hour. Plate was washed with wash buffer (1X) and 100µl TMB substrate (3,3',5,5'-Tetramethylbenzidine) solution was added and incubated in dark for 30 minutes. To stop the reaction, 100 µl of stop solution was added to each well and read the absorbance at 450 nm within 30 minutes.

Protein Expression Analysis with ELISA – IL-10

Experiment was performed as per kit instructions (Rat Interleukin 10, IL-10 GENLISA™ ELISA, CAT No.- KLR0108) 50 μl/well of diluted detection antibody were added to the plate. Plate was sealed and incubated for 30 minutes at 37°C. Plate was washed four times with wash buffer (1X) and buffer was blotted by firmly tapping plate upside down on absorbent paper. 100µl diluted Streptavidin -HRP solution was added to each well, plate was sealed and incubated for 30 minutes at 37°C. Plate was washed with wash buffer (1X) and 100µl TMB substrate (3,3',5,5'-Tetramethylbenzidine) solution was added and incubated in dark for 30 minutes. To stop the reaction, 100 µl of stop solution was added to each well and read the absorbance at 450 nm within 30 minutes.

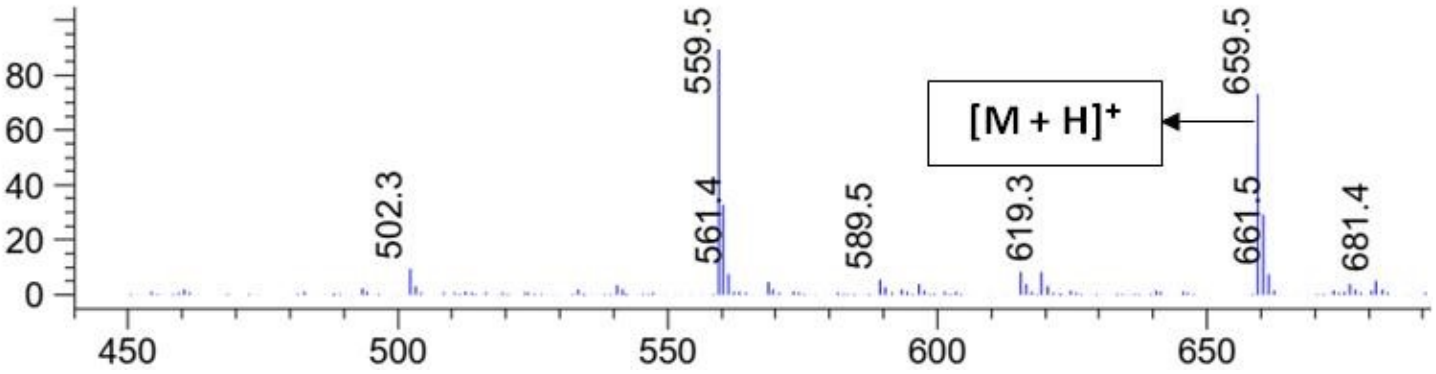

Figure S-2: - Mass Spectra of Hydrogelator **VIII**

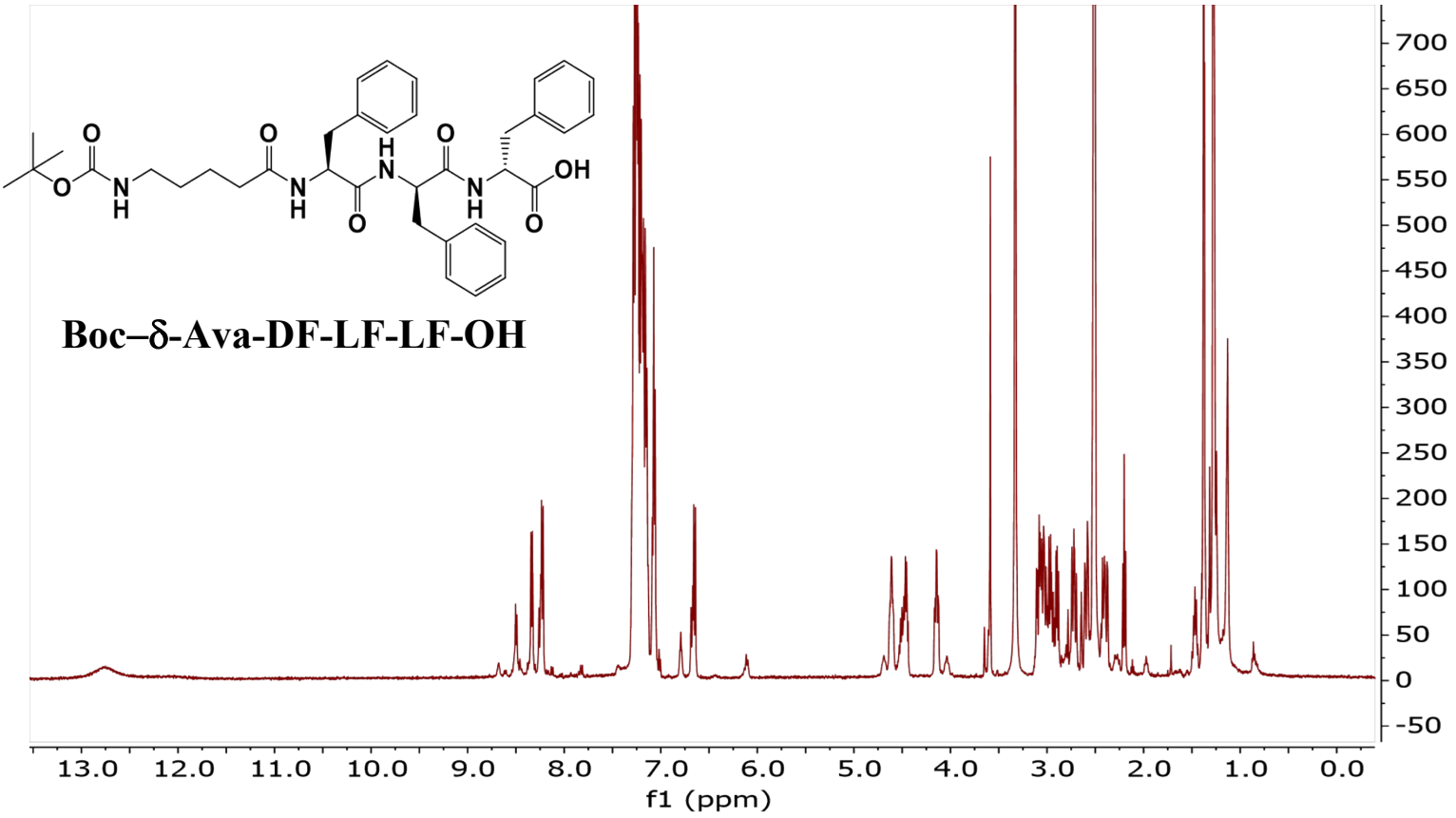

Figure S-3 (A): - ^{1}H NMR of **Hydrogelator VIII**

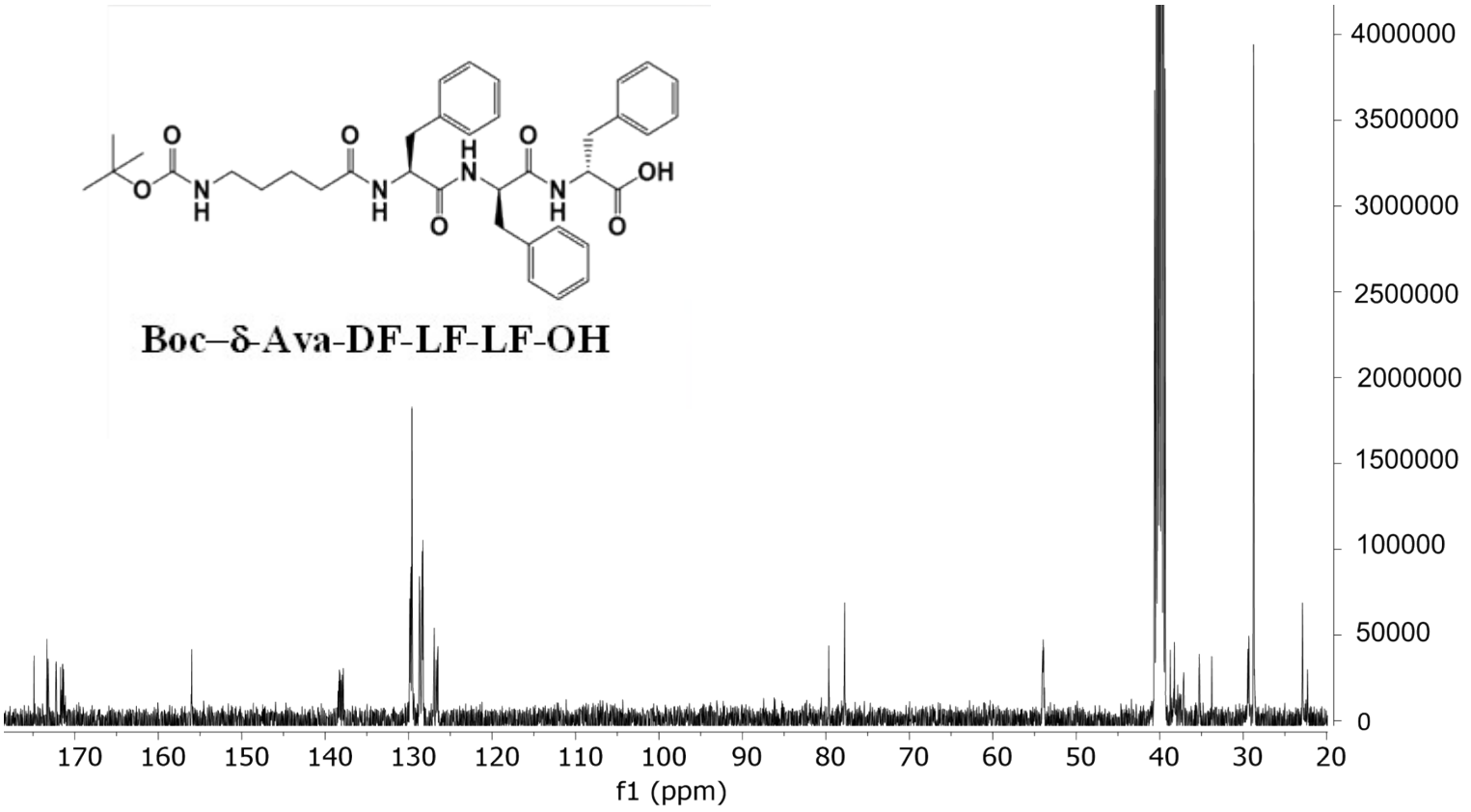

Figure S-3 (B): - ^{13}C NMR of **Hydrogelator VIII**

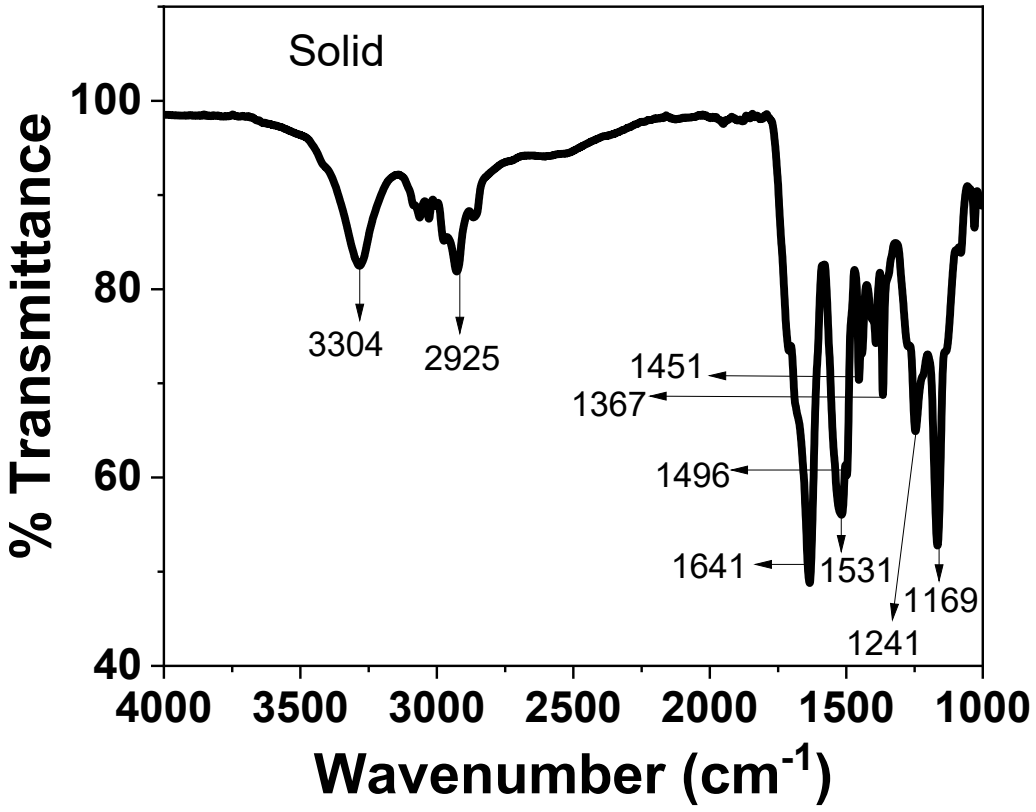

Figure S-4: - FTIR Study for Hydrogelator **VIII**

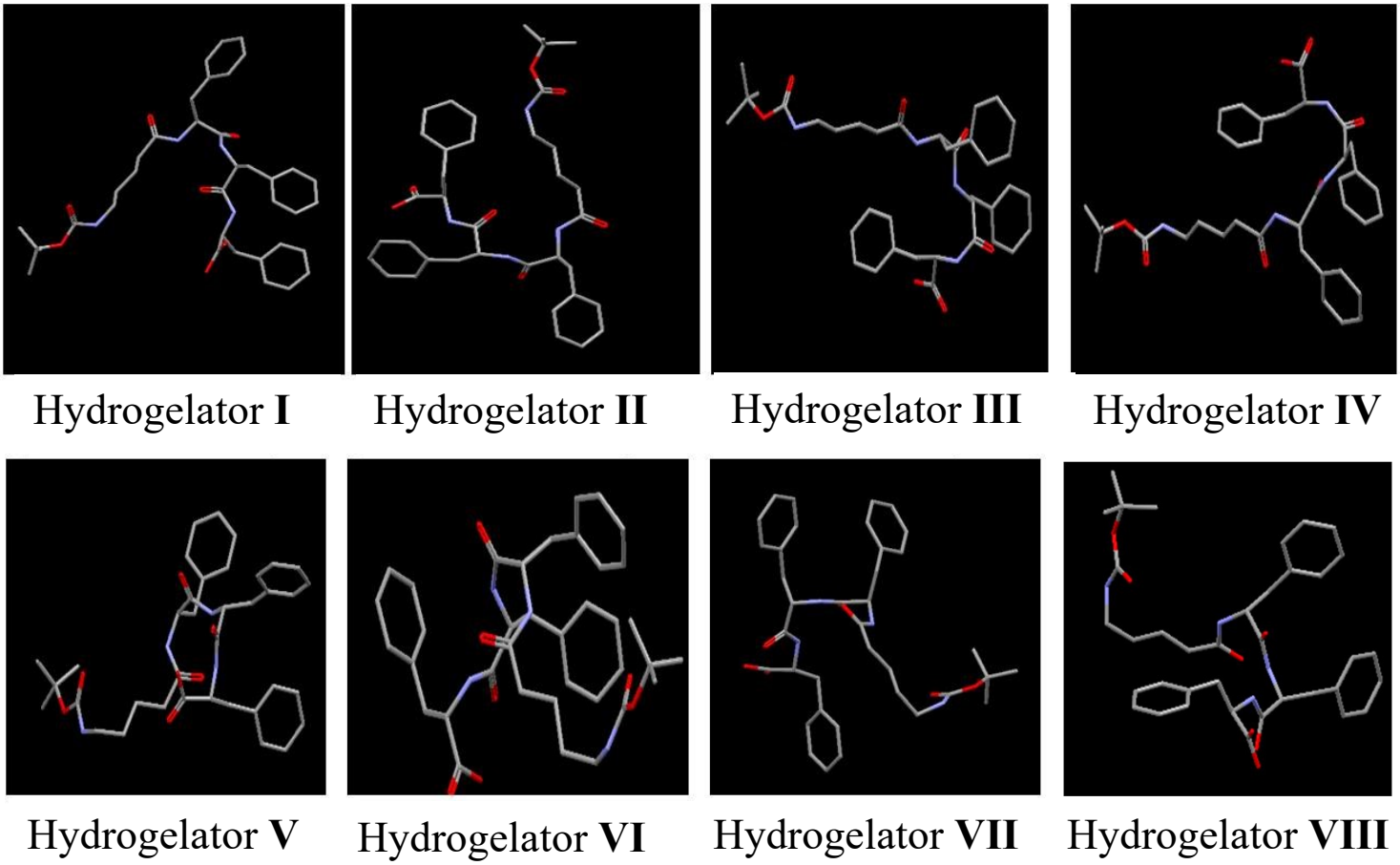

Figure S-5 (A): - Energy Optimized Structures for Hydrogelators **I - VIII**

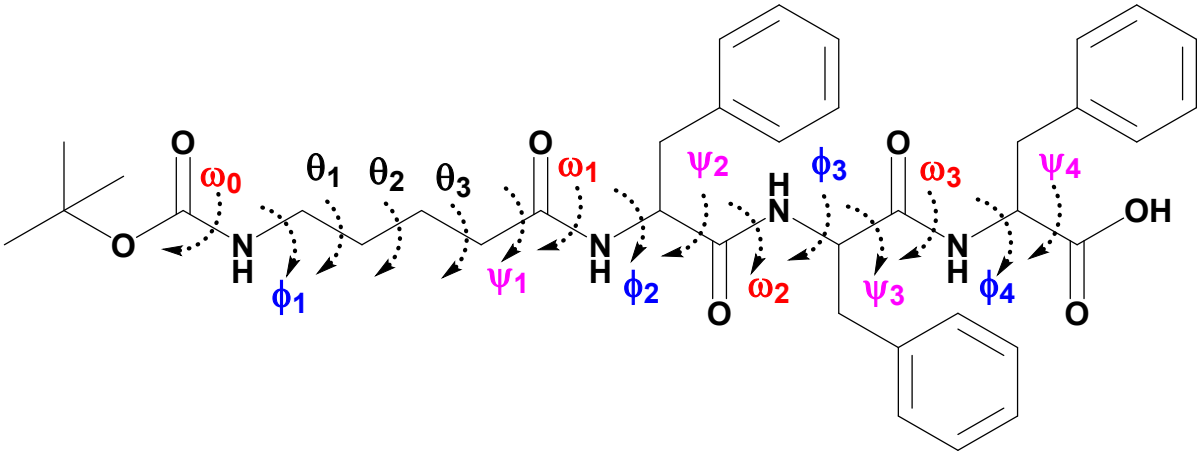

Figure S-5 (B): - Torsion Angles for Hydrogelators **I - VIII**

Table S1: - DFT Calculation and Torsion Angles for **Hydrogelators (I - VIII)**

S. No.	Torsion Angles	Hydrogelators							
		H-I LLL	**H-II LLD**	**H-III LDD**	**H-IV DDD**	**H-V DDL**	**H-VI LDL**	**H-VII DLD**	**H-VIII DLL**
1	ω_0	-175.8	178.85	178.44	-175.87	-177.19	178.36	179.19	-176.8
2	ϕ_1	-101.2	-81.46	-88.45	-92.92	-94.43	-110.94	-82.75	-93.47
3	θ_1	77.4	-178.39	-174.26	63.92	68.88	-178.86	-178.25	70.09
4	θ_2	-174.9	-177.61	178.04	176.52	-178.02	178.24	-177.41	-178.08
5	θ_3	-168.4	175.76	-175.69	179.23	-176.83	174.79	176.57	-169.9
6	ψ_1	-0.51	151.34	53.07	-0.77	-8.09	49.51	151.52	-5.19
7	ω_1	-174.11	174.28	173.21	-172.82	-178.99	175.07	-179.73	176.72
8	ϕ_2	-46.78	-156.82	-163.86	-73.99	-56.2	-164.75	143.43	-68.16
9	ψ_2	-43.31	-63.19	-60.67	55.77	131.63	-60.01	103.29	73.11
10	ω_2	-1.19	-162.89	153.65	-177.4	-179.4	154.25	162.99	-167.44
11	ϕ_3	126.65	155.32	-89.85	63.91	65.15	-91.02	51.98	97.11
12	ψ_3	-41.16	57.85	173.03	-57.67	-3.01	179.4	52.26	38.71
13	ω_3	-172.68	9.18	-180	175.63	-163.83	178.17	51.98	177.65
14	ϕ_4	69.03	120.78	170.5	75.19	142.61	111.04	137.5	67.89
15	ψ_4	124.8	11.6	-132.5	114.72	139.11	-1.8	14.26	116.28
16	**Relation b/w F_1-F_2**	Nearly Perpendicular	Parallel	Nearly Perpendicular	Nearly Parallel	Nearly Parallel	Perpendicular	Perpendicular	Nearly Perpendicular
17	**Relation b/w F_2-F_3**	Nearly Perpendicular	Nearly Perpendicular	Nearly Perpendicular	Opposite	Opposite	Parallel	Nearly Opposite	Nearly Perpendicular
18	**Relation b/w F_3-F_1**	Perpendicular	Perpendicular	Nearly Parallel	Nearly Perpendicular	Perpendicular	Nearly Parallel	Perpendicular	Perpendicular
19	**Log P**	2.11	2.44	1.8	2.144	2.133	2.028	2.8	1.272
20	**Zero point Vibrational Energy**	2091.0228 kJ mol^{-1}	2088.6668 kJ mol^{-1}	2086.7068 kJ mol^{-1}	2088.3098 kJ mol^{-1}	2093.1134 kJ mol^{-1}	2094.2328 kJ mol^{-1}	2092.7661 kJ mol^{-1}	2095.1366 kJ mol^{-1}
21	**Final Energy**	-2182.7299 a.u.	-2182.7131 a.u.	-2182.7131 a.u.	-2182.6976 a.u.	-2182.7262 a.u.	-2182.7329 a.u.	-2182.7261 a.u.	-2182.7366 a.u.

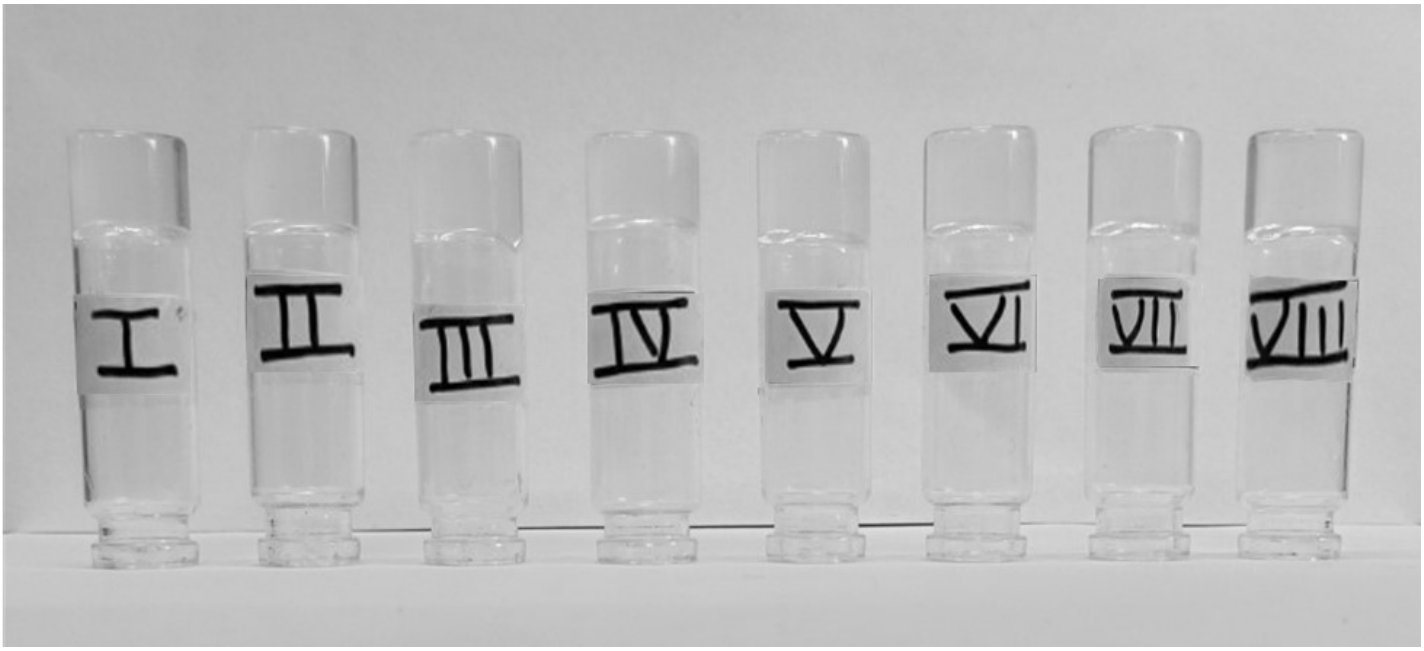

Figure S-6: - Gel Images of Hydrogelators **(I - VIII)**

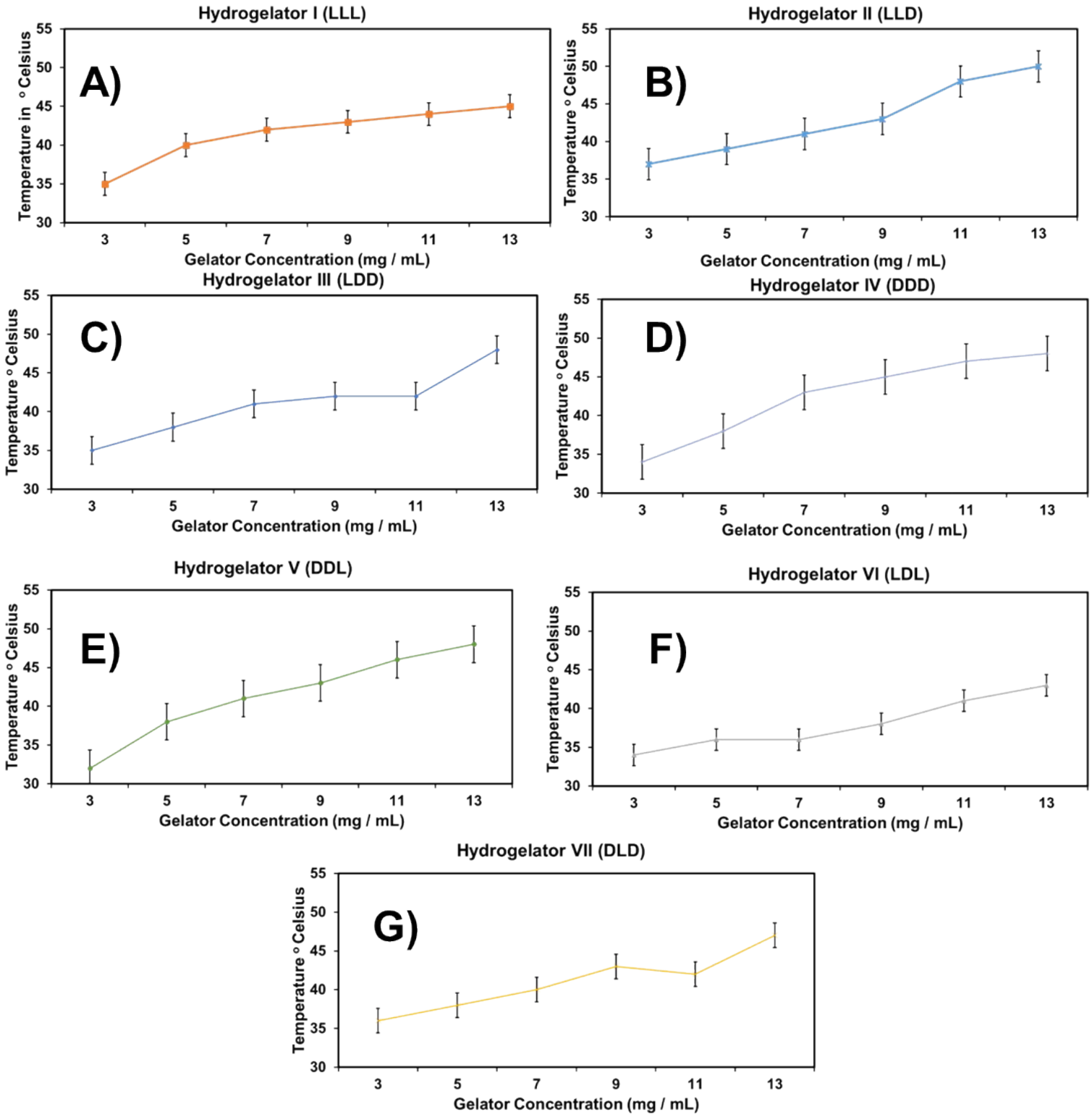

Figure S-7 (A): - T_{gel} and Gelator Concentration for Hydrogelators **(I - VII)**

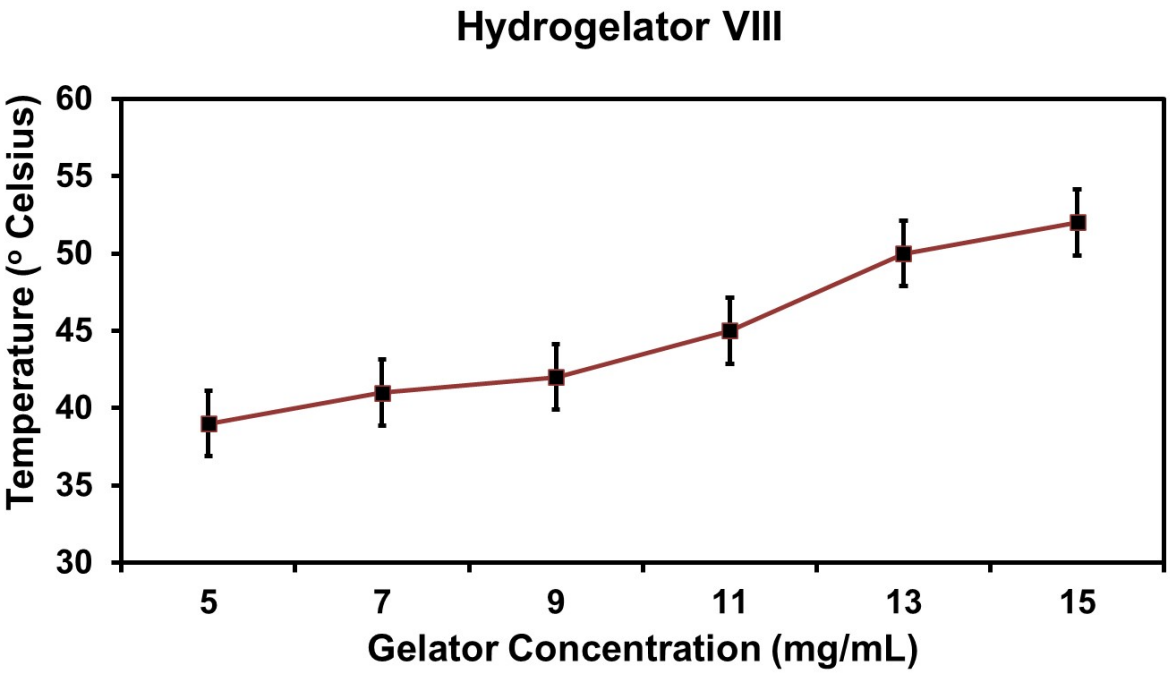

Figure S-7 (B): - T_{gel} and Gelator Concentration for Hydrogelator **VIII**

Figure S-7 (C): - Gel images of Hydrogelator **VIII ((i)** pH = 4.2**; (ii)** pH = 7.2 and **(iii) No gel formation at** pH = 9.2**)**

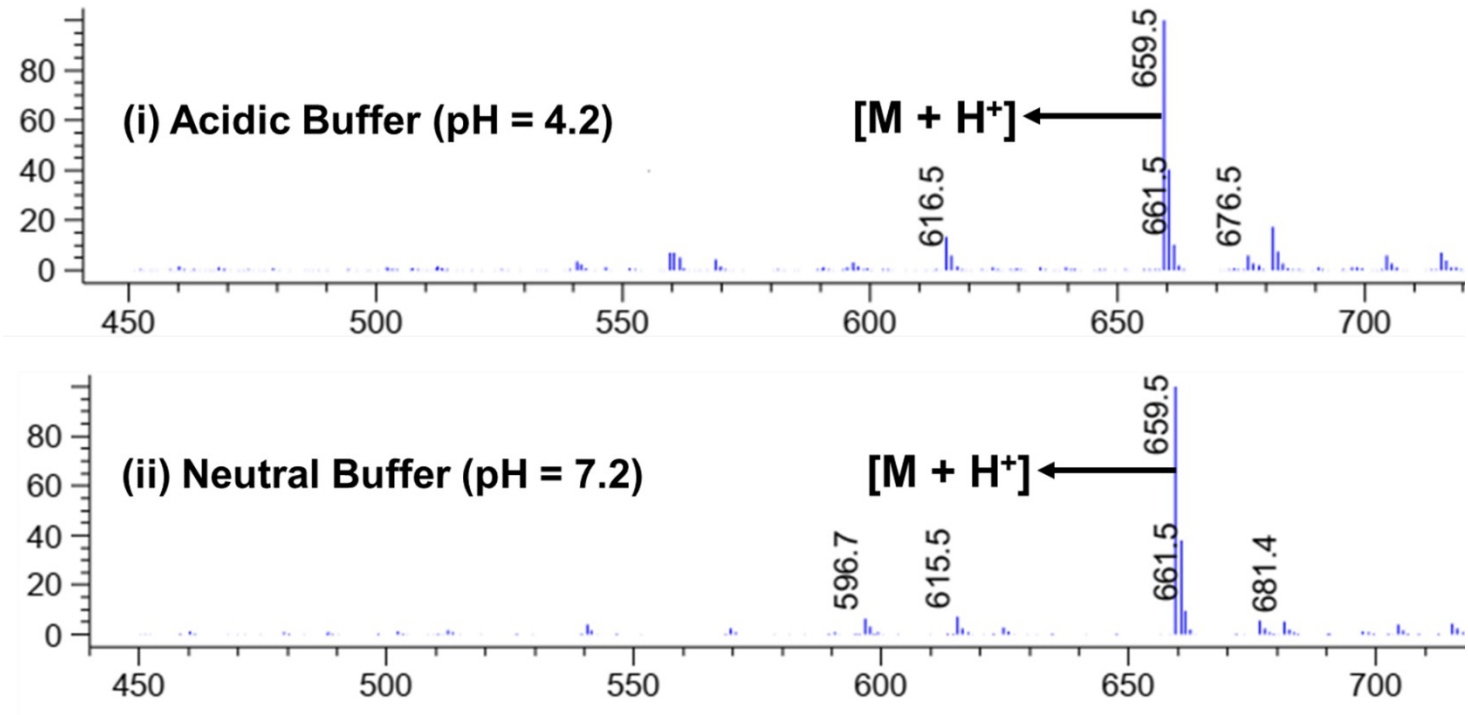

Figure S-7 (D): - Mass Spectra of Hydrogelator **VIII** Gels in **(i)** Acidic Buffer, gel taken from **(Fig. 7(C) (i))** and **(ii)**7.5 Phosphate Buffer, gel taken from **(Fig. 7(C)**

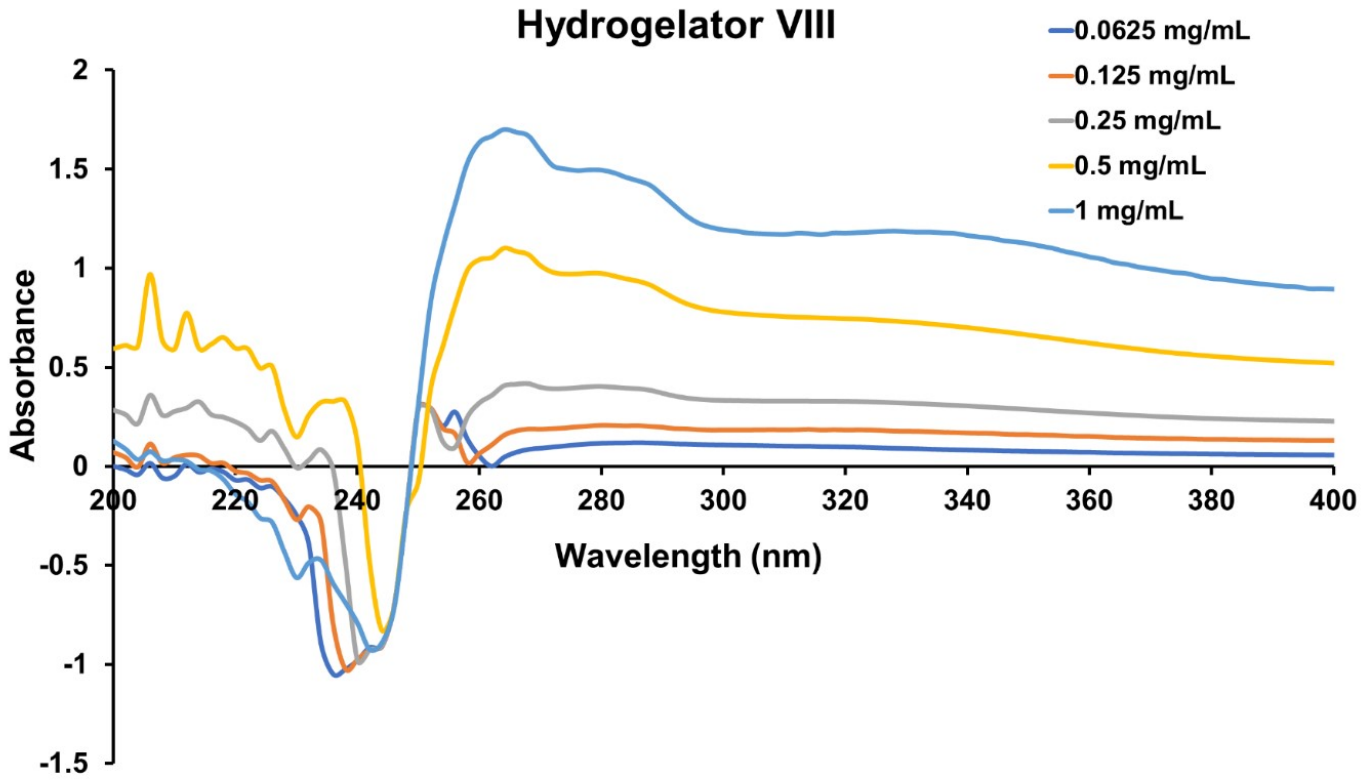

(ii))

Figure S-7 (E): - Concentration Dependent UV Studies of Hydrogelator **VIII** demonstrating no change in stability of the molecule with change in concentration as consistent pattern was obtained

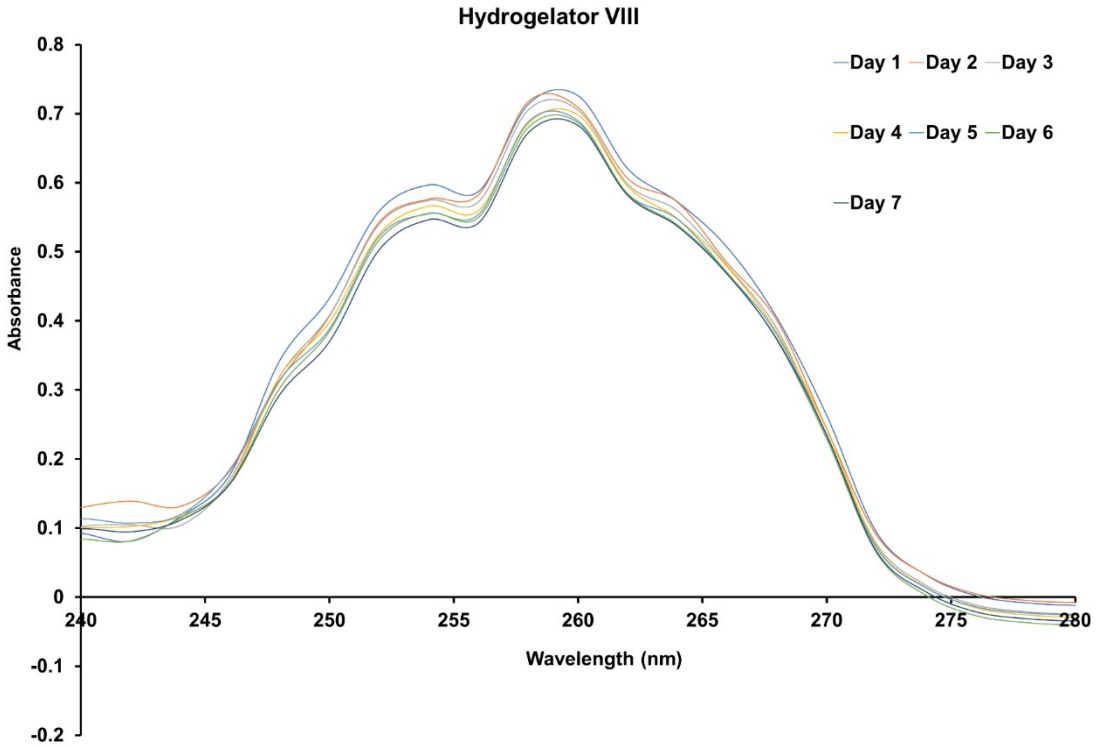

Figure S-7 (F): - UV Studies of Hydrogelator **VIII** demonstrating no change in stability of the molecule until 7 days as consistent pattern was obtained.

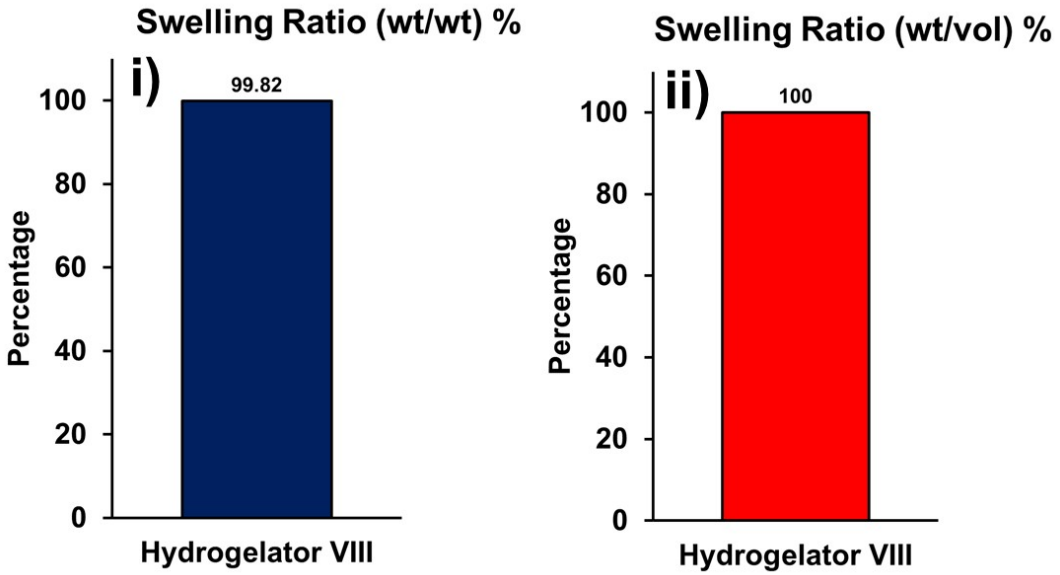

Figure S-7 (G): - Swelling Ratio of Hydrogelator **VIII**

Table – S2: - Data of Anti-inflammatory Assay for Hydrogelators **(I - VIII)**

S.No.	Hydrogelator	MMP-2	MMP-9
1.	Positive Control	100	95
2.	Negative Control	0	0
3.	Hydrogelator I (LLL)	62	52
4.	Hydrogelator II (LLD)	50	45
5.	Hydrogelator III (LDD)	58	30
6.	Hydrogelator IV (DDD)	60	35
7.	Hydrogelator V (DDL)	57	31
8.	Hydrogelator VI (LDL)	55	43
9.	Hydrogelator VII (DLD)	50	35
10.	Hydrogelator VIII (DLL)	94	92

Table – S3 : - Data of Hydrogelator **VIII** Dilutions

S.No.	Hydrogelator VIII DILUTIONS (µg/mL)	Anti-inflammatory activity against MMP-2(% inhibition)
1.	PC	97.44
2.	NC	0
3.	0.97	96.44
4.	1.95	97.44
5.	3.9	94.43
6.	7.81	97.44
7.	15.6	95.43
8.	31.25	97.44
9.	62.5	95.43
10.	125	96.44
11.	250	96.44
12.	500	95.43
13.	100	100.46

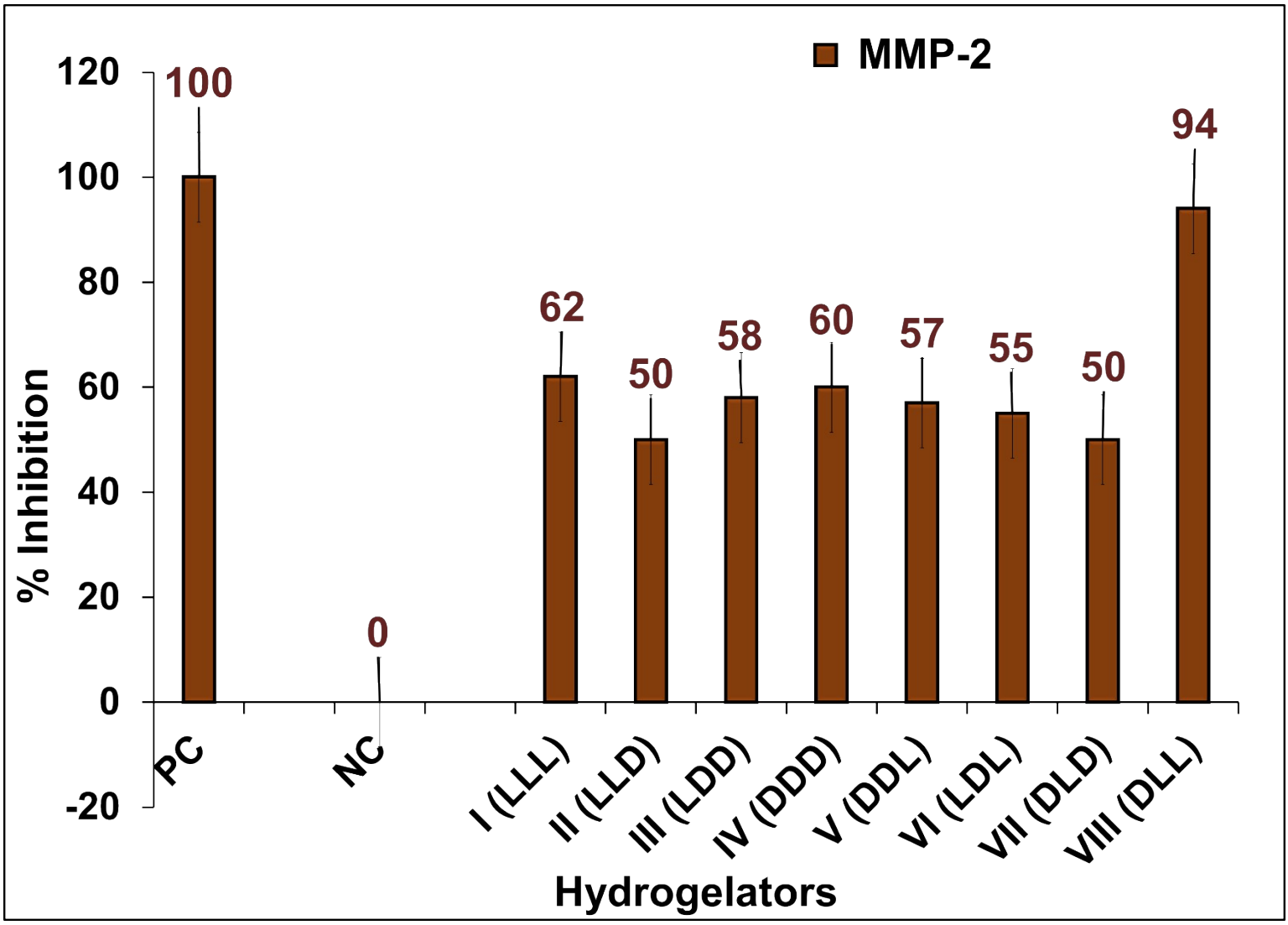

Figure S-8: - Percentage inhibition studies of Hydrogelators (**I-VIII)**

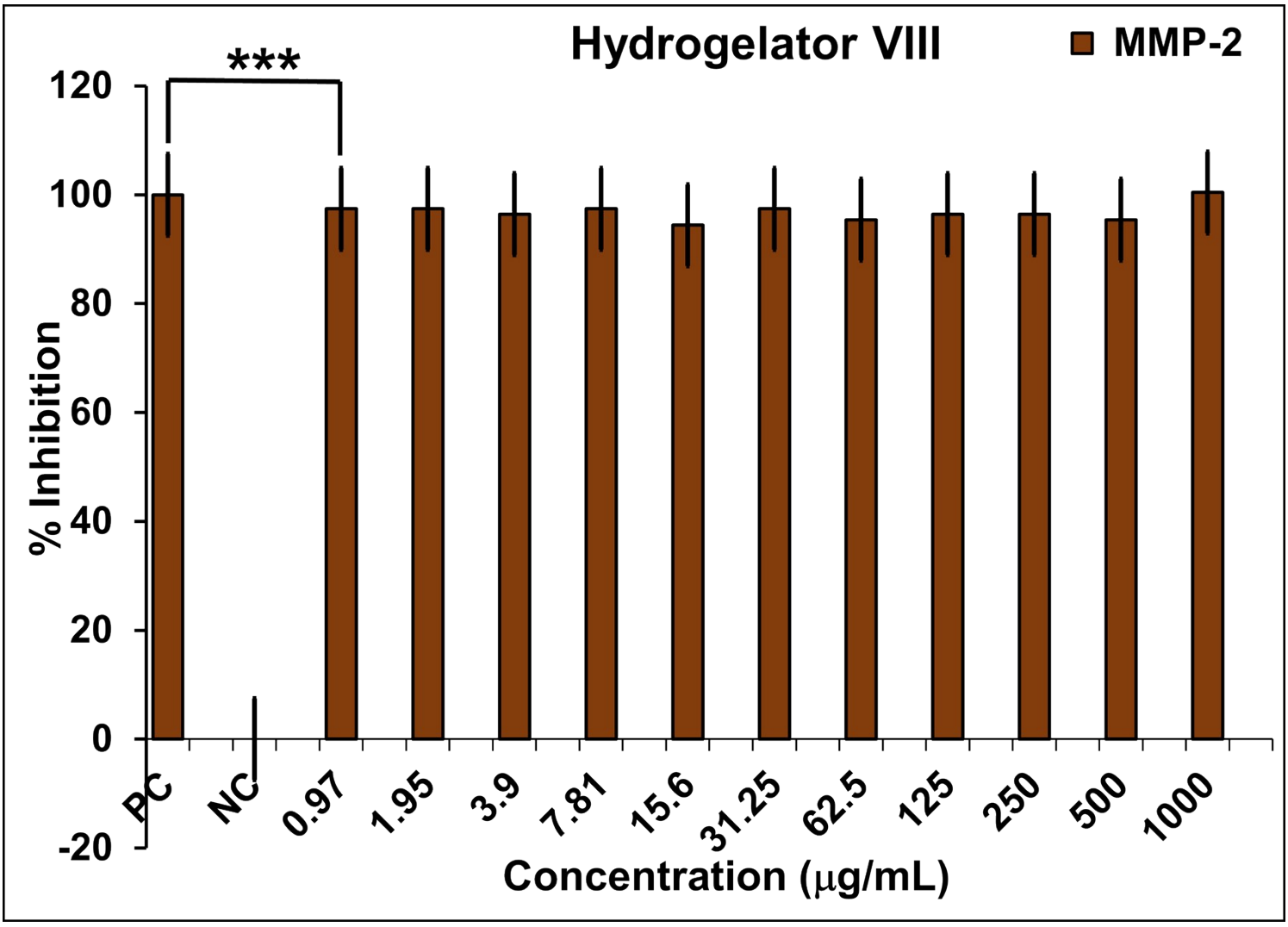

Figure S-9: - Concentration dependent anti-inflammatory activity of Hydrogelator **VIII.** Data was statistically analysed using a two-tailed paired Student's t test and presented as mean ± SD (N = 3). ***$p < 0.001$, as compared to the positive control group.

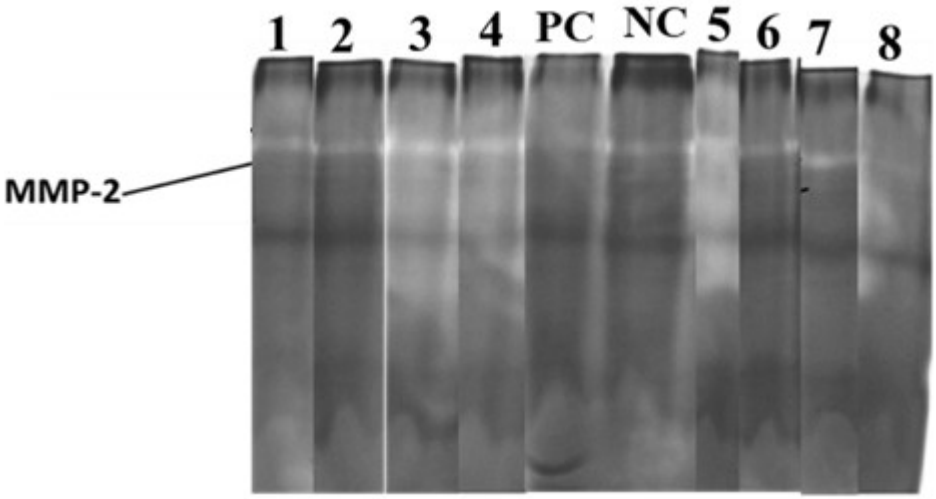

1. Hydrogelator **I (LLL)**
2. Hydrogelator **II (LLD)**
3. Hydrogelator **III (LDD)**
4. Hydrogelator **IV (DDD)**
   Positive Control (PC)
   Negative Control (NC)
5. Hydrogelator **V (DDL)**
6. Hydrogelator **VI (LDL)**
7. Hydrogelator **VII (DLD)**
8. Hydrogelator **VIII (DLL)**

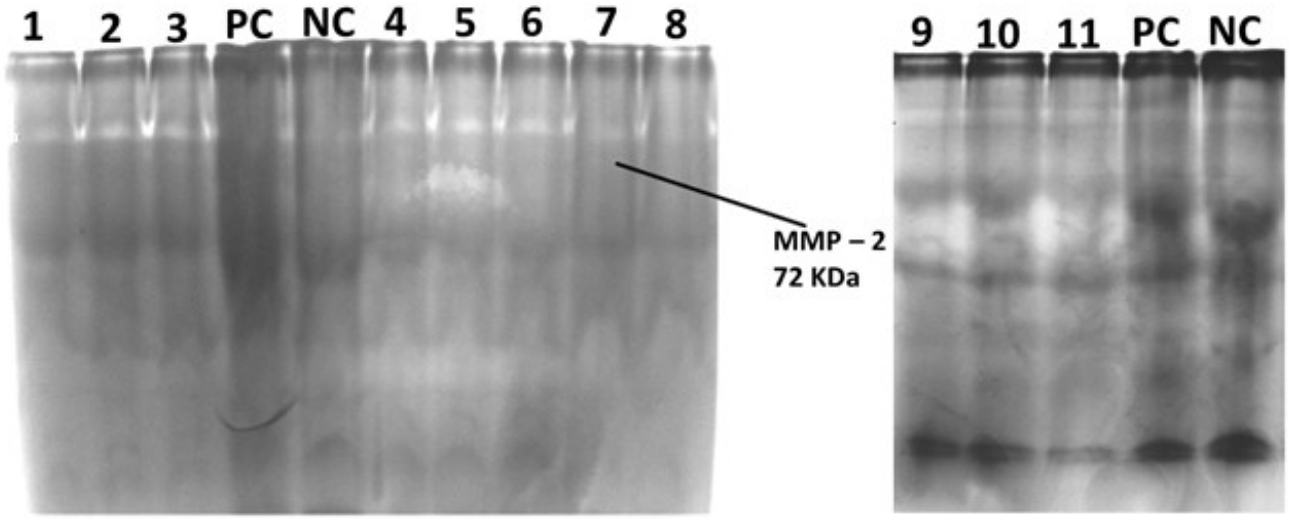

1. 1000 μg/mL
2. 500 μg/mL
3. 250 μg/mL

PC - Positive Control
NC – Negative Control

4. 125 μg/mL
5. 62.5 μg/mL
6. 31.25 μg/mL
7. 15.6 μg/mL
8. 7.81 μg/mL

9. 3.90 μg/mL
10. 1.5 μg/mL
11. 0.97 μg/mL

PC - Positive Control
NC – Negative Control

Figure S-10: - Gelatin Zymography of Hydrogelators **(I- VIII)**

Figure S-11: - Gelatin Zymography for dilutions of Hydrogelator **VIII**

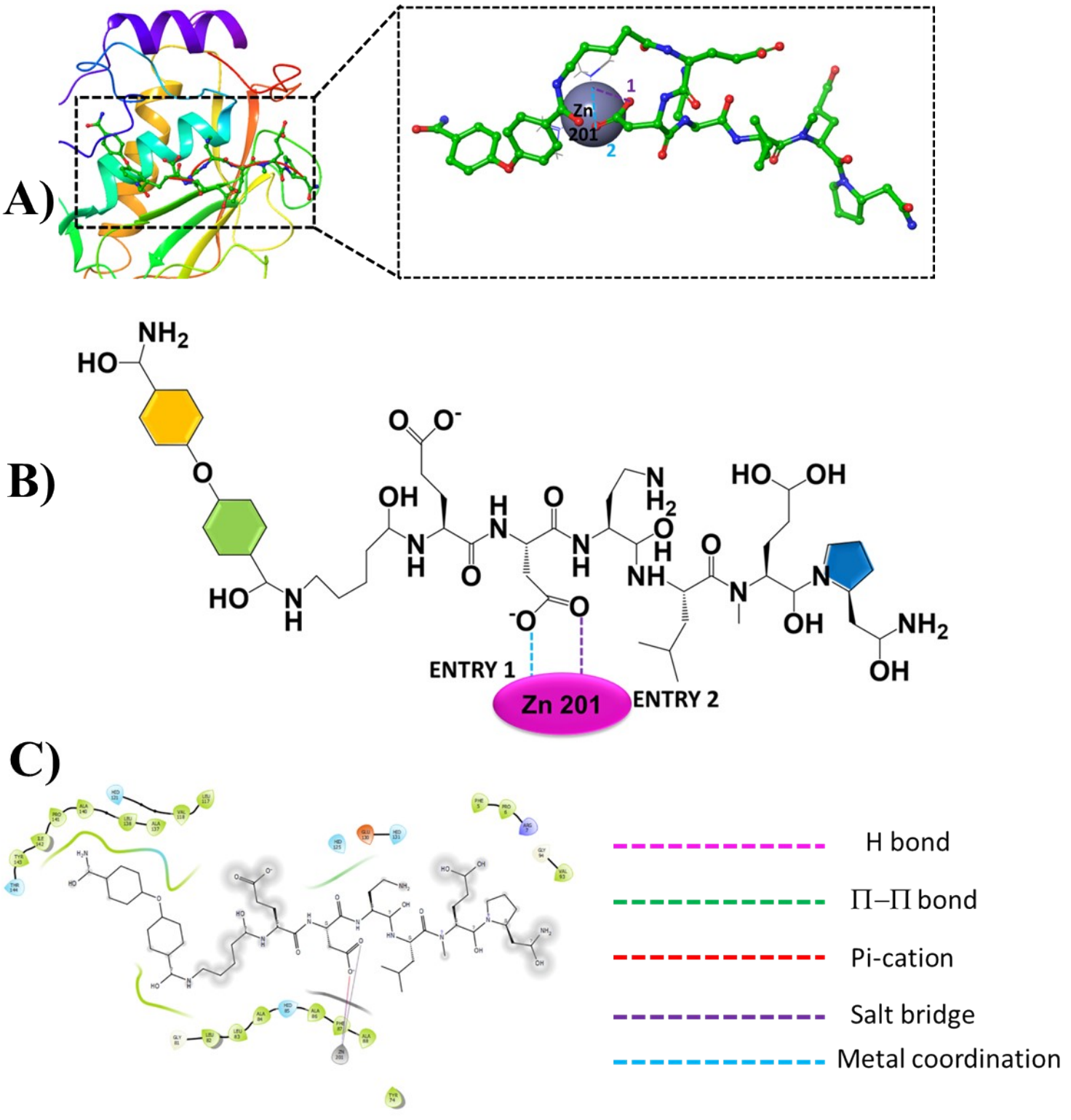

Figure S-12:

A) 3D representation of the mode of interactions in Co-crystallized ligand

B) Pictorial diagram of the mode of interactions of Co-crystallized ligand, Aryloxy phenylcarboxamide-heptapeptide (heptapeptide: Glu-Asp-Gln-Leu-NMe-Glu-Pro)

C) 2D representation of the mode of interactions in Co-crystallized ligand

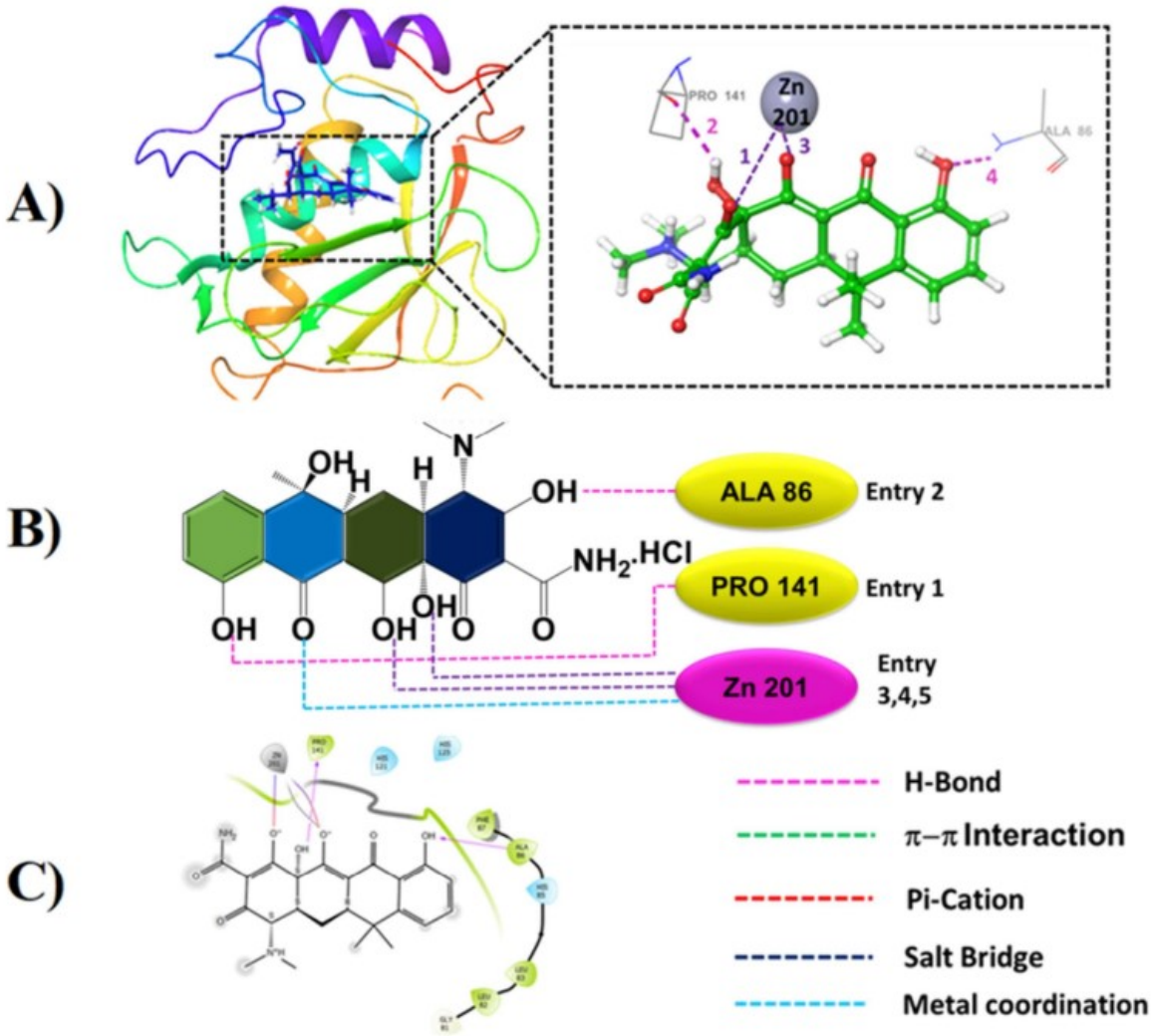

Figure S-13:

A) 3D representation of the mode of interactions in Reference ligand
B) Pictorial diagram of the mode of interactions of Reference ligand, Tetracycline Hydrochloride
C) 2D representation of the mode of interactions in Reference ligand.

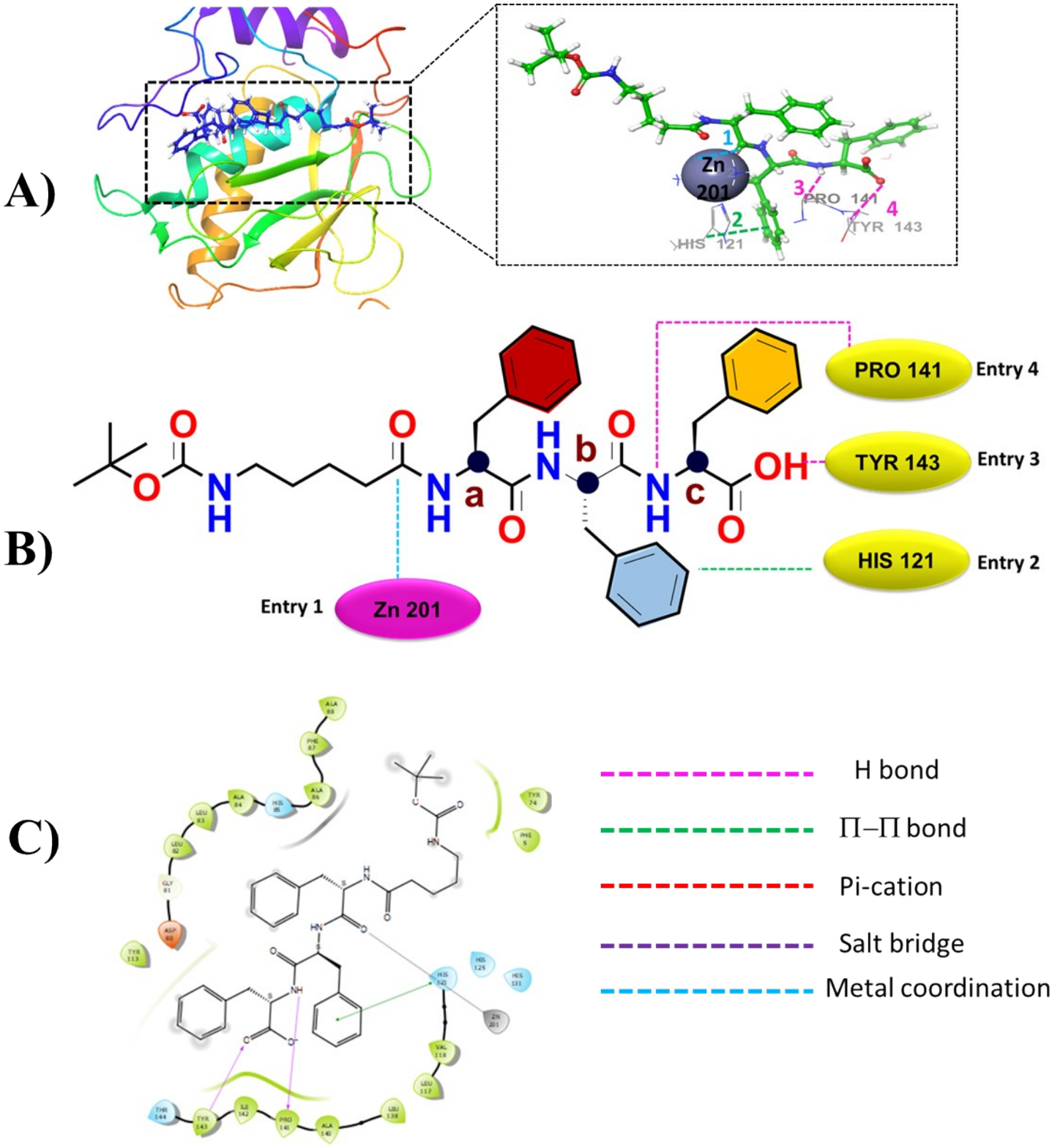

Figure S-14:

A) 3D representation of the mode of interactions in Hydrogelator **I**
B) Pictorial diagram of the mode of interactions of Hydrogelator **I**
C) 2D representation of the mode of interactions in Hydrogelator **I**

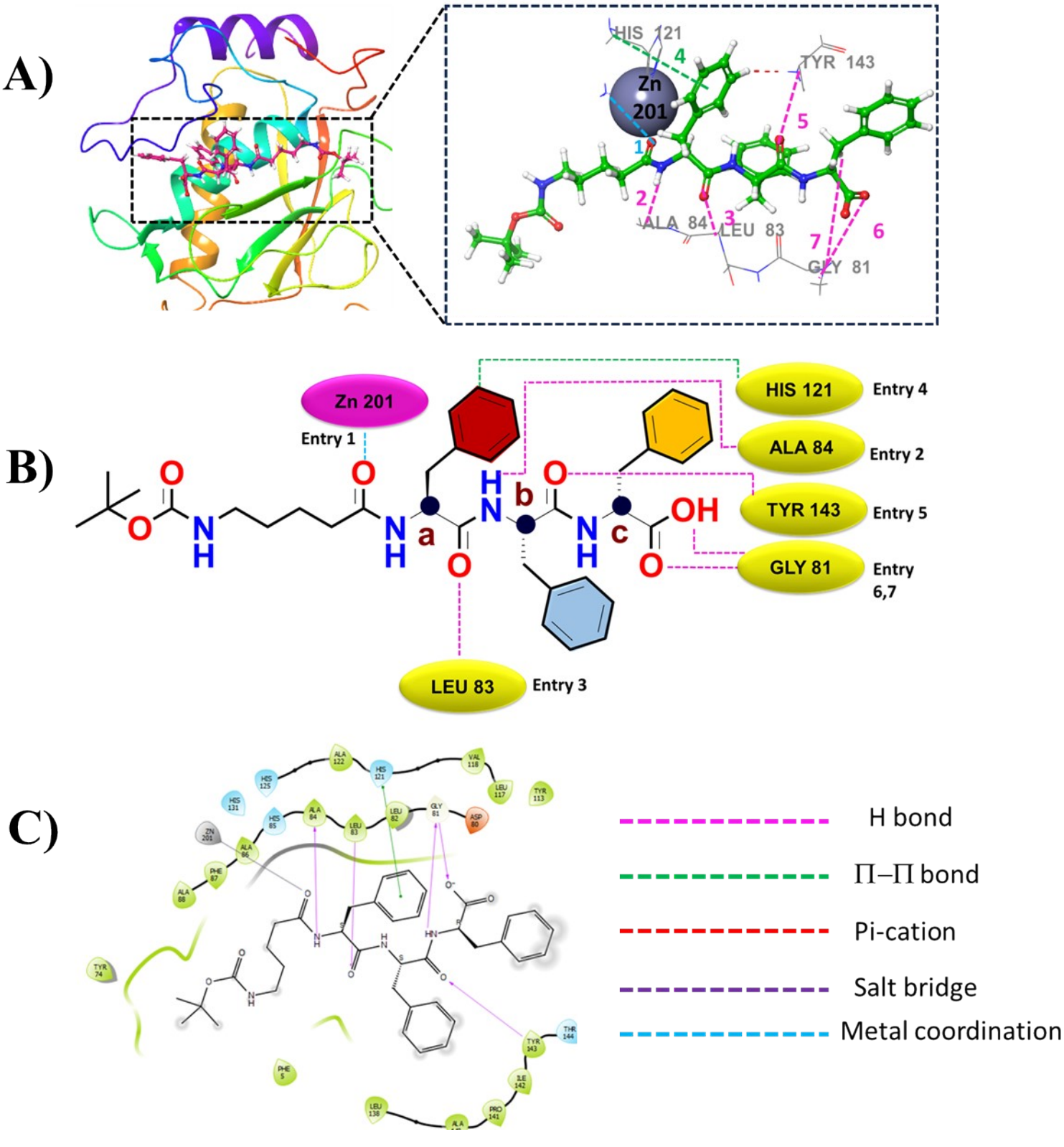

Figure S-15:

A) 3D representation of the mode of interactions in Hydrogelator **II**
B) Pictorial diagram of the mode of interactions of Hydrogelator **II**
C) 2D representation of the mode of interactions in Hydrogelator **II**

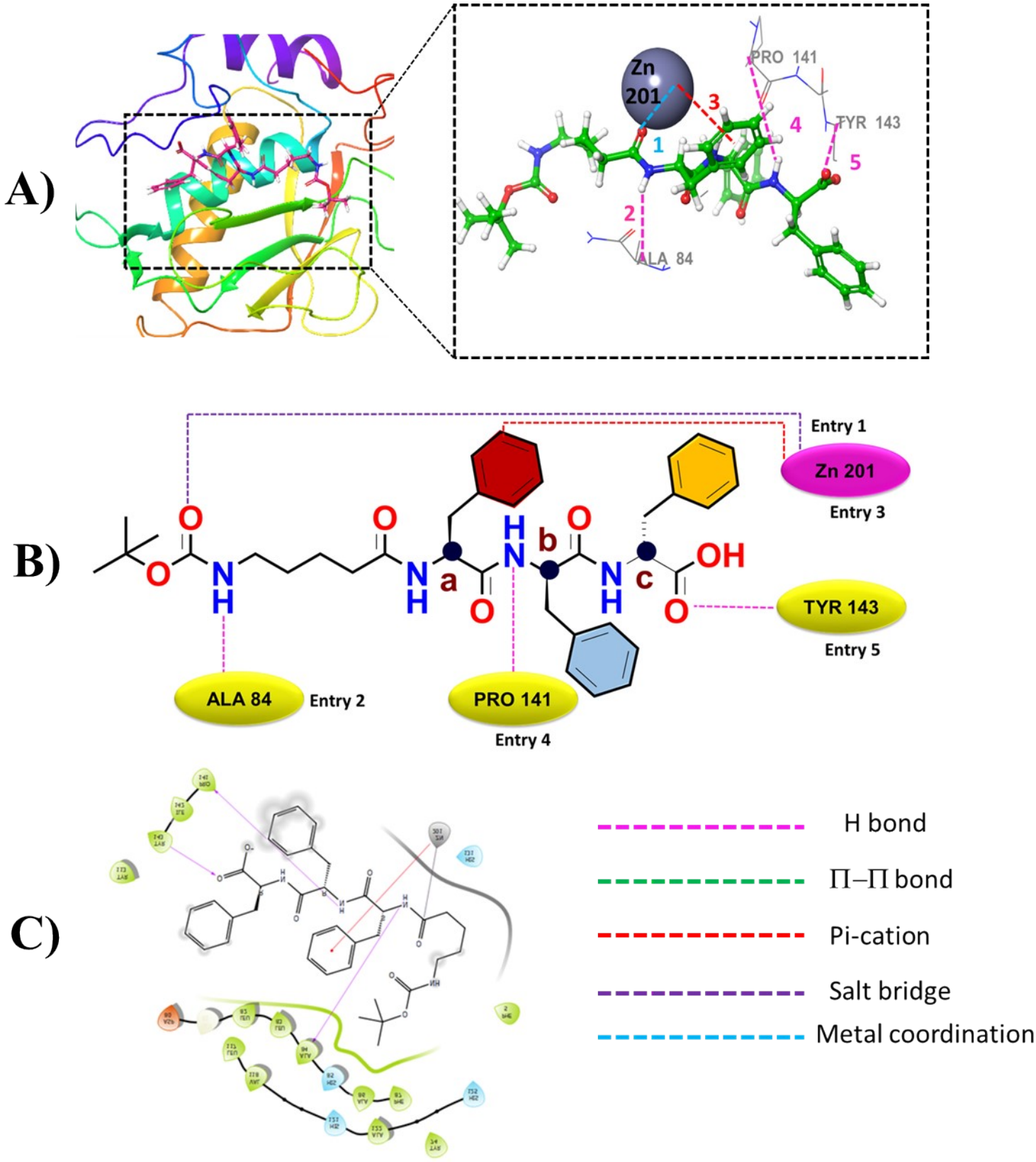

Figure S-16:

A) 3D representation of the mode of interactions in Hydrogelator **III**
B) Pictorial diagram of the mode of interactions of Hydrogelator **III**
C) 2D representation of the mode of interactions in Hydrogelator **III**

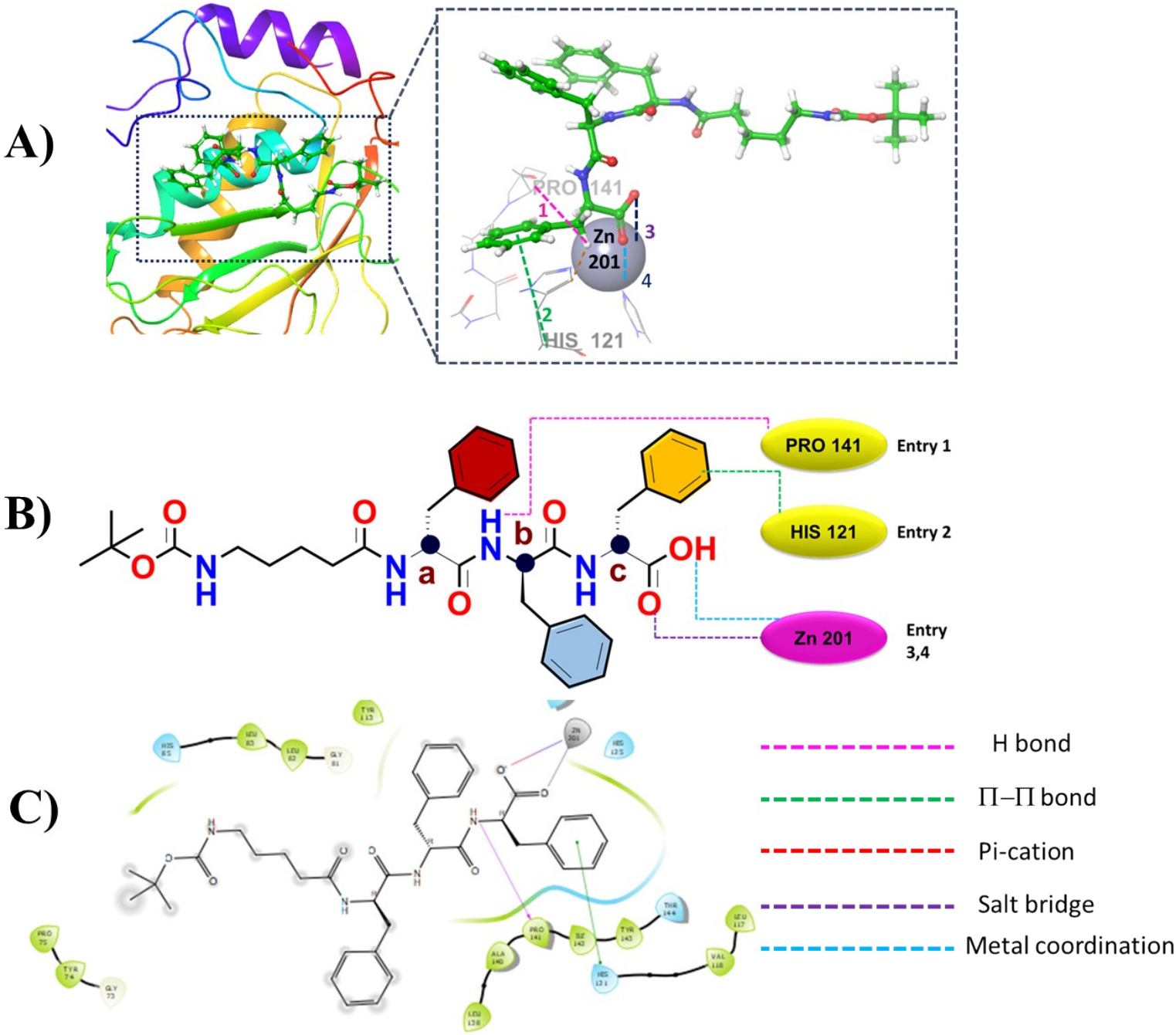

Figure S-17:

A) 3D representation of the mode of interactions in Hydrogelator **IV**
B) Pictorial diagram of the mode of interactions of Hydrogelator **IV**
C) 2D representation of the mode of interactions in Hydrogelator **IV**

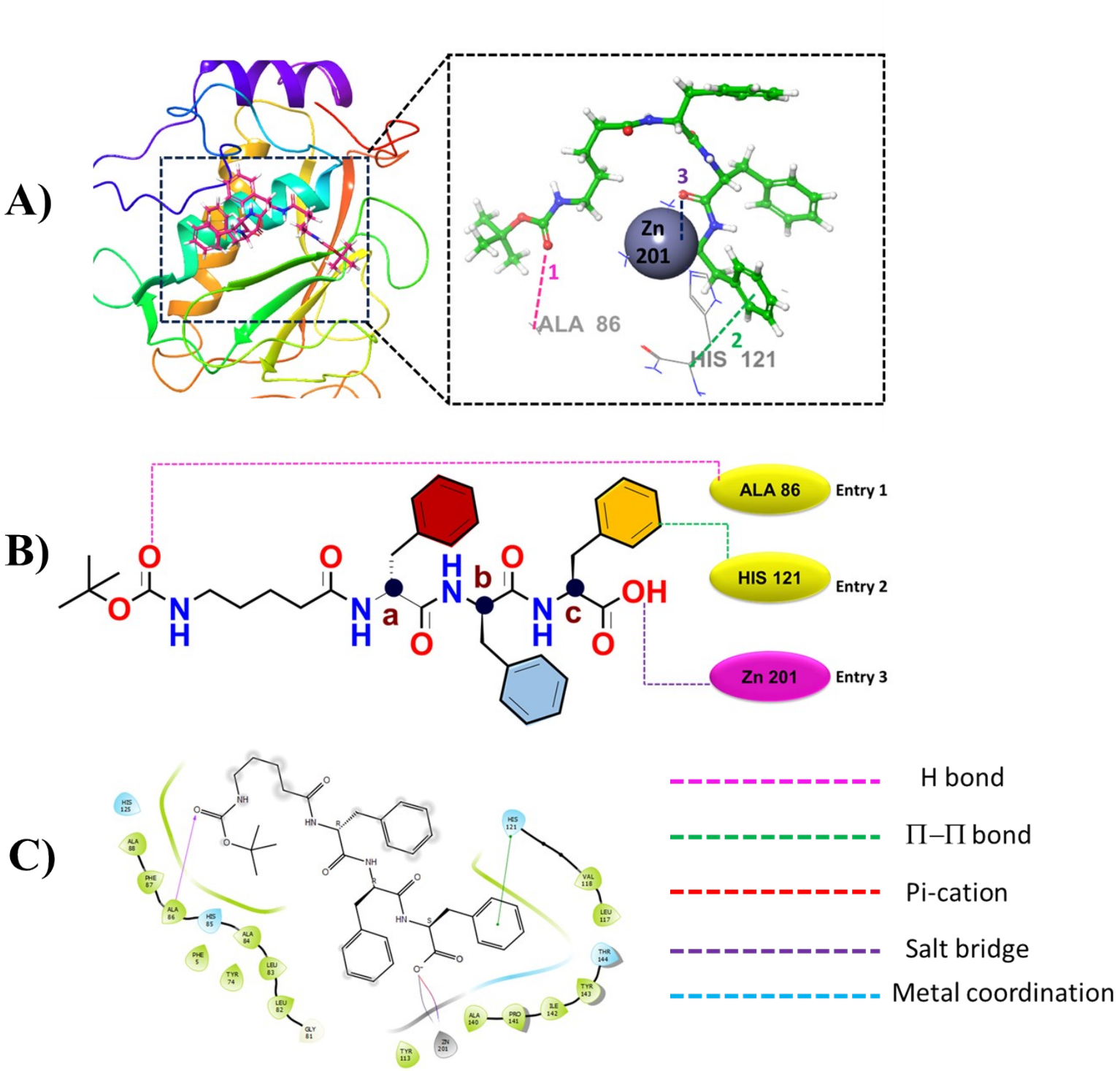

Figure S-18:

A) 3D representation of the mode of interactions in Hydrogelator **V**
B) Pictorial diagram of the mode of interactions of Hydrogelator **V**
C) 2D representation of the mode of interactions in Hydrogelator **V**

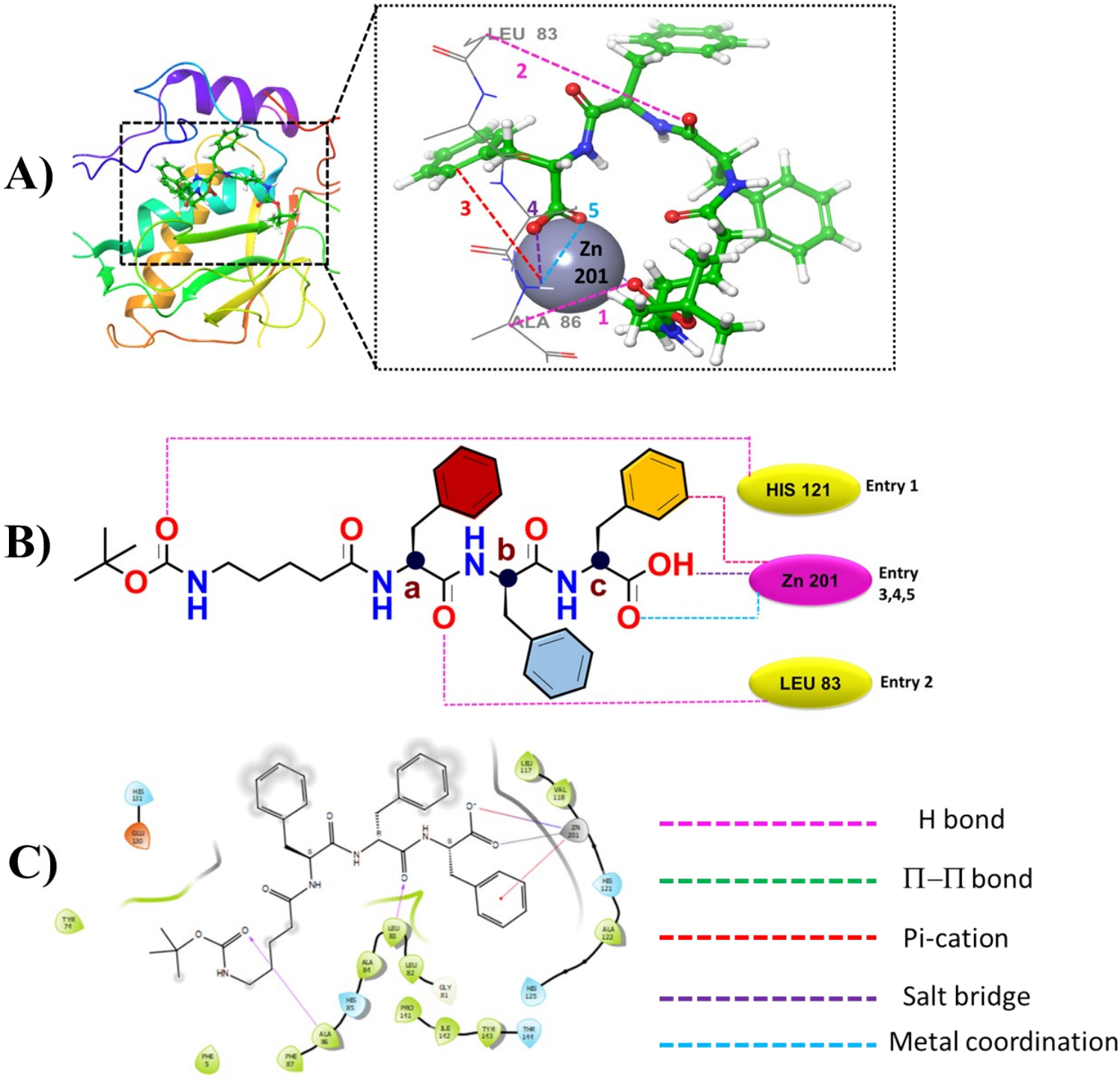

Figure S-19:

A) 3D representation of the mode of interactions in Hydrogelator **VI**
B) Pictorial diagram of the mode of interactions of Hydrogelator **VI**
C) 2D representation of the mode of interactions in Hydrogelator **VI**

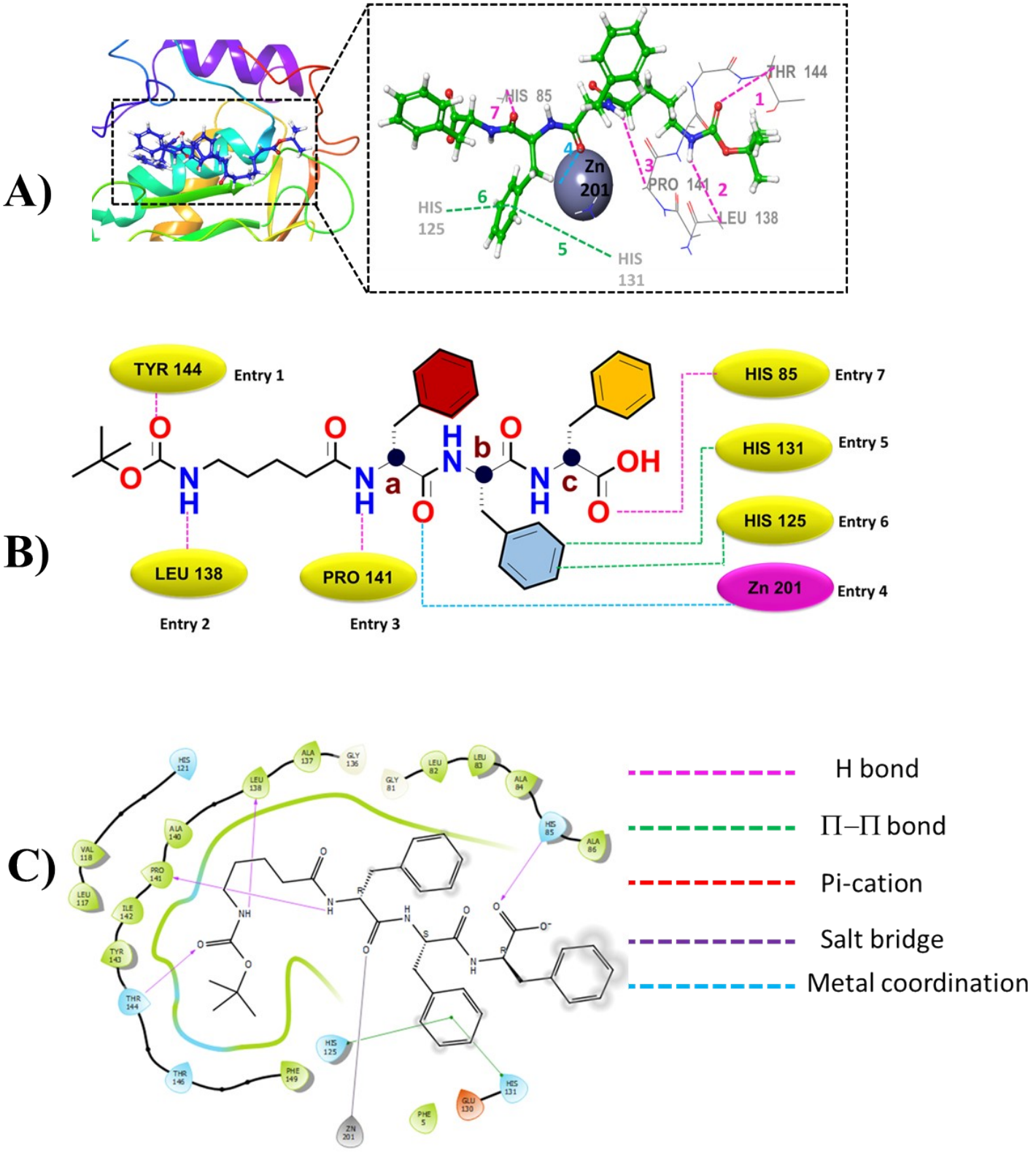

Figure S-20:

A) 3D representation of the mode of interactions in Hydrogelator **VII**
B) Pictorial diagram of the mode of interactions of Hydrogelator **VII**
C) 2D representation of the mode of interactions in Hydrogelator **VII**

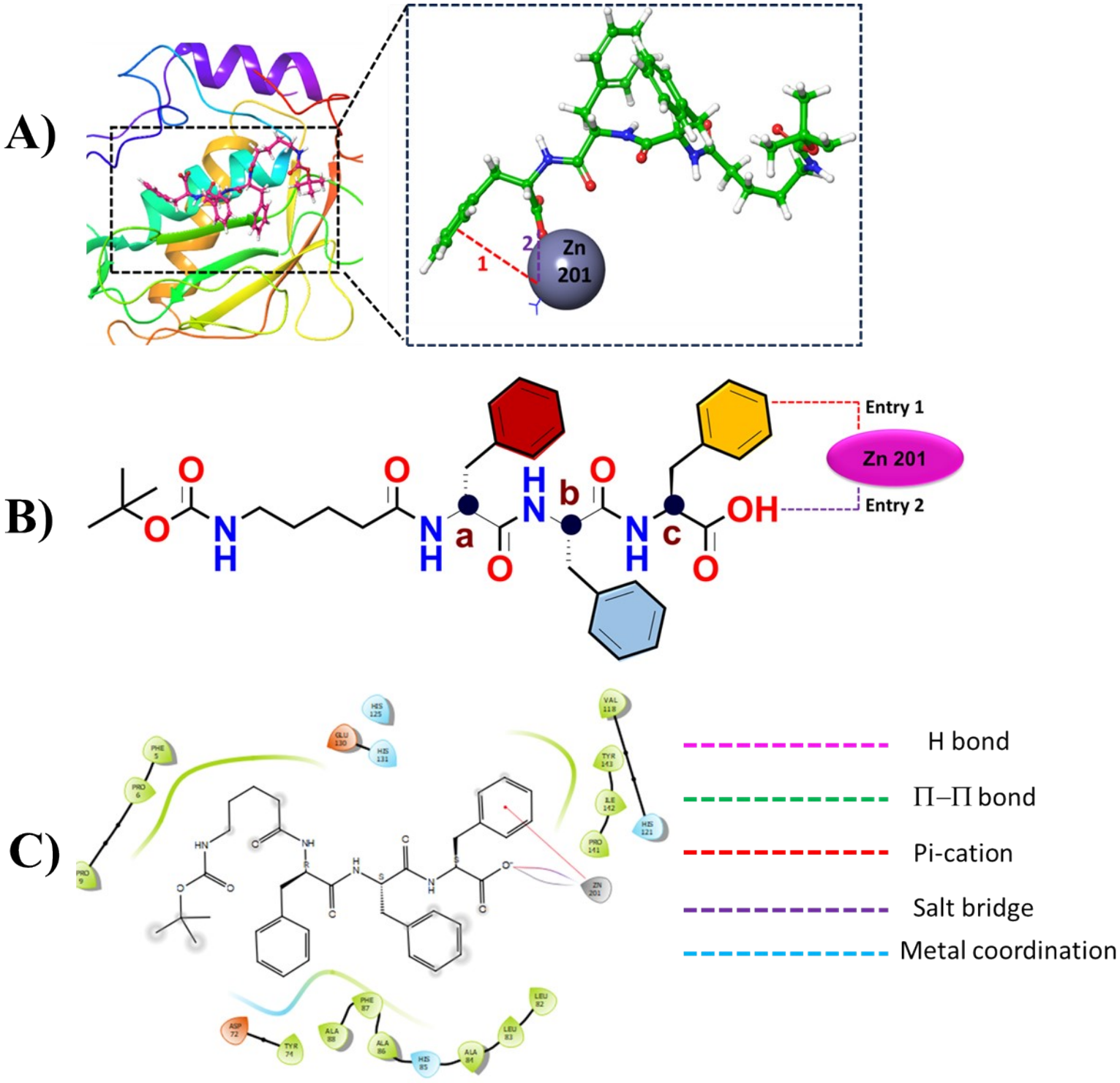

Figure S-21:

A) 3D representation of the mode of interactions in Hydrogelator **VIII**
B) Pictorial diagram of the mode of interactions of Hydrogelator **VIII**
C) 2D representation of the mode of interactions in Hydrogelator **VIII**

Table – S4 : - Various interactions of the Co-crystallized ligand, Tetracycline hydrochloride and Hydrogelator **I - VIII** with the receptor MMP2

Entry		**Nature of Interactions**	**Donor**	**Acceptor**
1	**Co-crystallized Ligand**	Salt bridge	O^- side chain carboxylate of Aspartic acid	Zn^{2+} (201)
2		Metal-co-ordination	Side chain carboxylate carbonyl of Aspartic acid	Zn^{2+} (201)
		Nature of Interactions	**Donor**	**Acceptor**
1		H-Bond	OH at the junction of the aromatic ring 1 and 2	Carbonyl Pro 141
2		H-Bond	OH of aromatic ring 4	Carbonyl Ala86
3	**Tetracycline Hydrochloride**	Salt bridge	O^- of aromatic ring 1	Zn^{2+} (201)
4		Salt bridge	O^- of aromatic ring 2	Zn^{2+} (201)
5		Metal Co-ordination	Zn 201	O^- of aromatic ring 3
		Nature of Interactions	**Donor**	**Acceptor**
1		Metal coordination	Zn 201	Phe(1) CO
2		π-π	Phe(2)aromatic ring	His 121 aromatic ring
3	**Hydrogelator I**	H-bond	Tyr 143 NH	Phe(3) O of carboxylate
4		H-bond	Phe(3) NH	Pro 141
		Nature of Interactions	**Donor**	**Acceptor**
1		Metal coordination	Zn 201	Ava(1) CO
2		H-bond	Phe(1) NH	Ala 84
3		H-bond	Leu 83	Phe(1) CO
4		π-π	Phe(1)aromatic ring	His 121 aromatic ring
5	**Hydrogelator II**	H-bond	Tyr 143 NH	Phe(2) CO
6		H-bond	Gly 81	Phe(3) $O^-$of carboxylate
7		H-bond	Phe (3) NH	Gly 81
		Nature of Interactions	**Donor**	**Acceptor**
1		Metal coordination	Ava CO	Zn 201
2		H-bond	Ava NH	Ala 84 CO
3	**Hydrogelator III**	Pi-cation	Phe (1)	Zn 201
4		H-bond	Phe (1) NH	Pro 141
5		H-bond	Phe (3) CO	Zn 201
		Nature of Interactions	**Donor**	**Acceptor**
1		H-bond	Phe (3) NH	Pro141 CO
2		π-π	Phe(3)aromatic ring	HIS 121
3	**Hydrogelator IV**	Salt bridge	Zn 201	O^- of ring 3
4		Metal coordination	O^- of ring 3	Zn 201
		Nature of Interactions	**Donor**	**Acceptor**
1		H-bond	Ala 86	BOC -CO
2	**Hydrogelator V**	π-π	Phe (3) o- carboxylate	His 121
3		Salt bridge	Phe (3) o- carboxylate	Zn 201

		Nature of Interactions	Donor	Acceptor
1		H-bond	Boc -CO	Ala 86
2		H-bond	Phe(1) CO	Leu 83
3		Pi-cation	Phe (3) aromatic ring	Zn 201
4	Hydrogelator VI	Salt bridge	Zn 201	O^- of ring 3
5		Metal coordination	CO of ring 3	Zn 201
		Nature of Interactions	**Donor**	**Acceptor**
1		H-bond	Thr 144	BOC- CO
2		H-bond	Boc- NH	Leu 138
3		H-bond	δ-Ava NH	Pro 141
4		Metal coordination	Zn 201	Phe (1) CO
5	Hydrogelator VII	π-π	Phe(2) aromatic ring	His 131
6		π-π	Phe(2) aromatic ring	His 125
7		H-bond	His 85	Phe (3) CO
		Nature of Interactions	**Donor**	**Acceptor**
1	Hydrogelator VIII	Salt bridge	Carboxylate OH of Phe(3)	Zn^{2+} (201)
2		Pi-cation	Phe(3) aromatic ring	Zn^{2+} (201)

S. No.	Organism	MIC (μg/mL)
1.	*S. mutans*	0.4
2.	*S. aureus*	0.4
3.	*B. subtilis*	0.4
4.	*E.fecalis*	0.4
5.	*P. aeruginosa*	50
6.	*Proteus spp.*	Inactive
7.	*E. coli*	100
8.	*Klebsiella pneumoniae*	100

Table S5 : - Data of Antibacterial Assay for Hydrogelator **VIII**

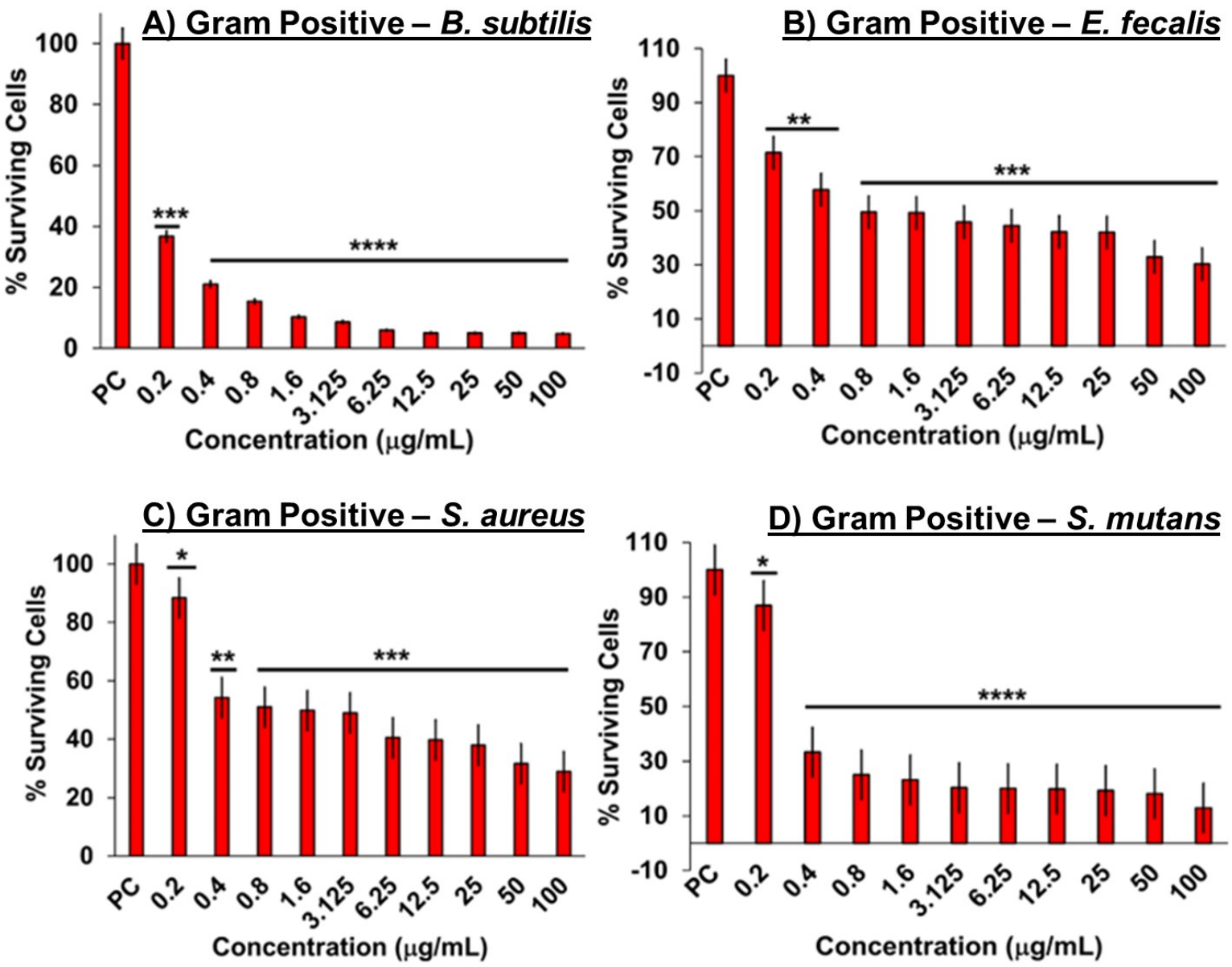

Figure S-22 (A-D): - Antibacterial Assay (Gram Positive Bacteria) for Hydrogelator **VIII.** Data was statistically analysed using a two-tailed paired Student's t test and presented as mean ± SD (N = 3). *$p < 0.05$, **$p < 0.01$, ***$p < 0.001$, ****$p < 0.0001$, as compared to the positive control group.

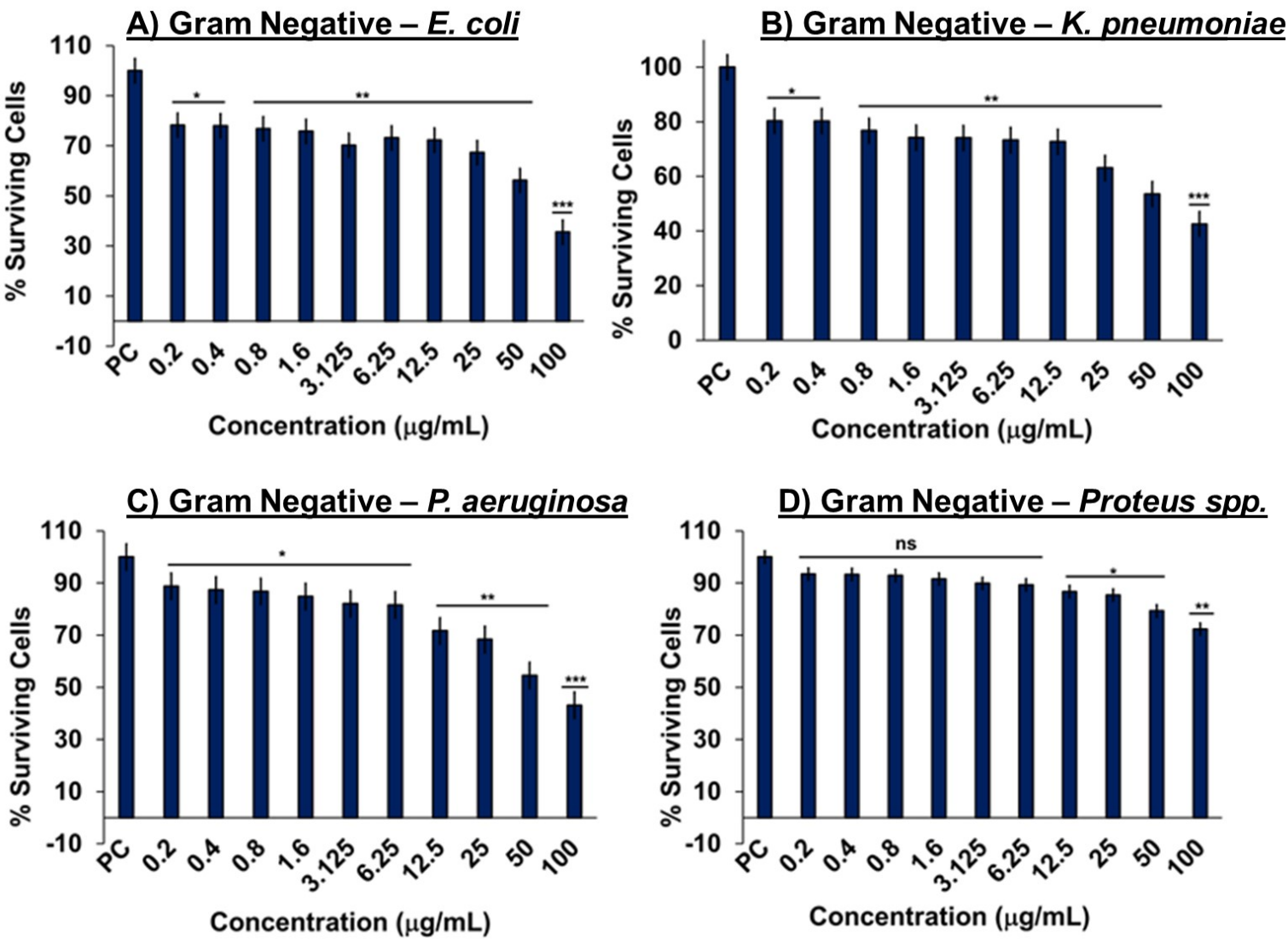

Figure S-22 (G-H): - Antibacterial Assay (Gram Negative Bacteria) for Hydrogelator **VIII.** Data was statistically analysed using a two-tailed paired Student's t test and presented as mean ± SD (N = 3). ns = not Significant,*$p < 0.05$, **$p < 0.01$, ***$p < 0.001$, as compared to the positive control group.

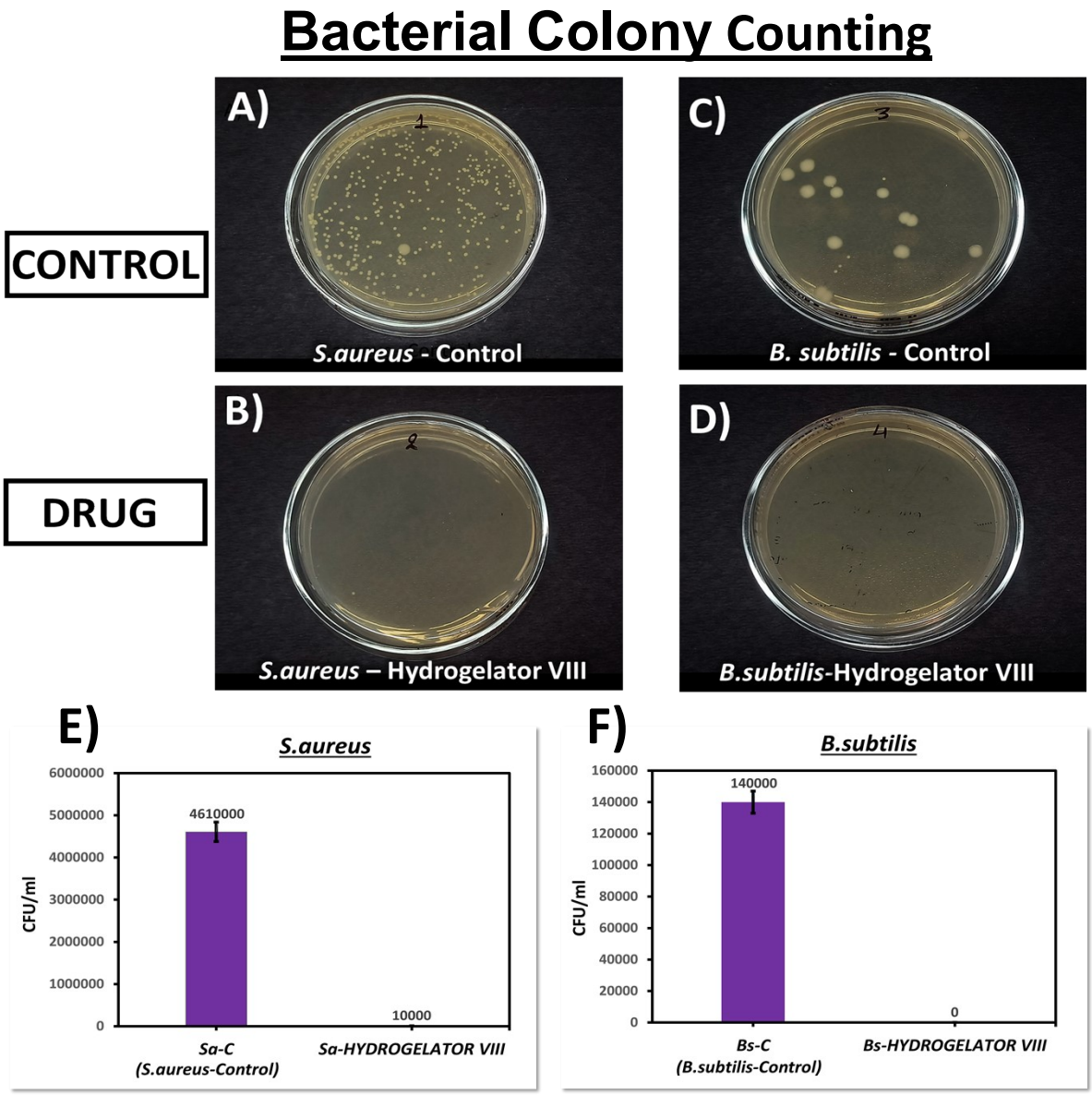

Figure S-23 (A-F): Enlarged image of Colony counting experiment of Hydrogelator VIII in two different bacteria: *S. aureus*; A) Control B) Treated one; *B. subtilis*; C) Control D) Treated one; E) and F) showing the net change in colony forming units per ml with respect to the control in both the organisms.

Bacterial SEM

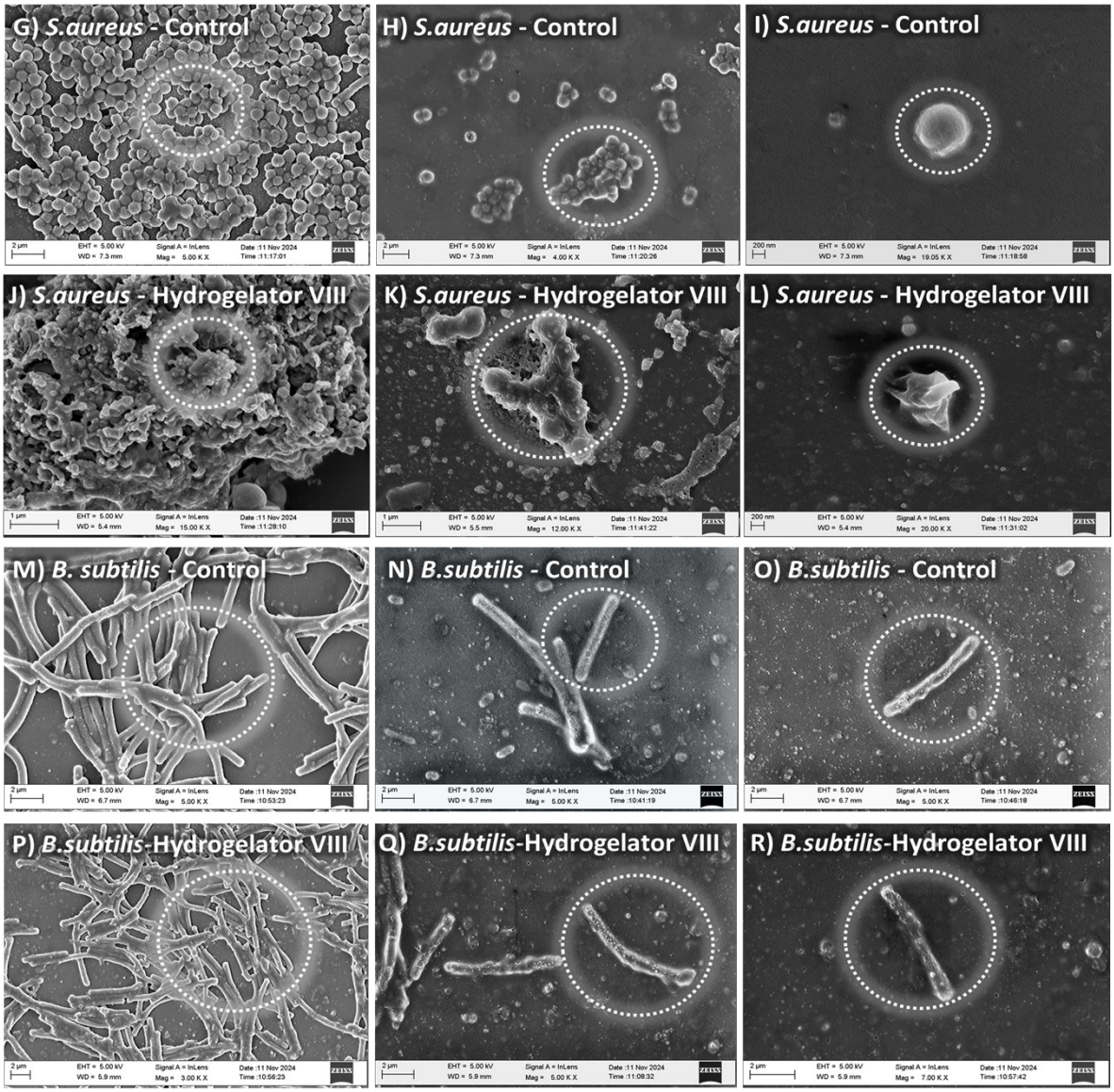

Figure S-24 (A-L): Enlarged FE-SEM Images of Hydrogelator **VIII**, induced membrane disruption of the bacterial cells. Hydrogelator **VIII** (2X MIC) incubated with *S. aureus*; Control (A-C) and treated with Hydrogelator **VIII** (D-F); *B. subtilis*; Control (G-I) and treated with Hydrogelator **VIII** (J-L)

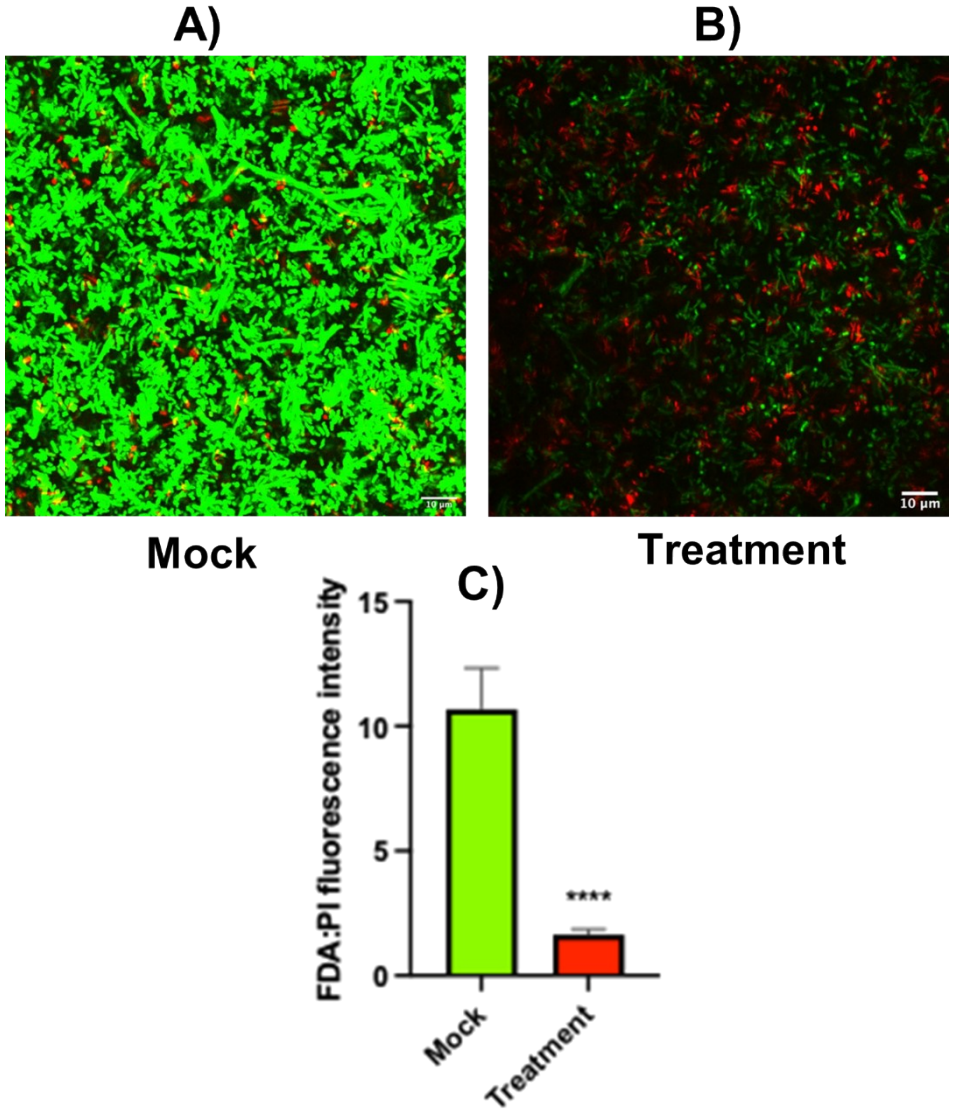

Figure S-25 (A-B) Representative images of viable *Bacillus subtilis* grown in mock (DMSO) and treatment (0.4ug/ml) for 24 hours at 37 degrees. The cell viability was tested using a combination of Fluorescein diacetate (FDA :1mg/ml) and Propidium Iodide (PI:2ug/ml). The cells were stained with FDA for 5mins followed by 1x PBS washes for 2mins. The cells were further stained with PI for 2mins followed by 1x PBS wash for 2mins twice. The cells were then visualised under a confocal microscope 40X objective using 488nm and 561nm excitation. For FDA and PI respectively.

(C) The plot represents a ratio of FDA:PI fluorescence intensities from both mock and treatment cells. The higher value indicates more viable cells whereas lower value indicates more dead cells. The result in the plot is of two biological replicates analysed with t-test for significance testing ($p<0.05$).

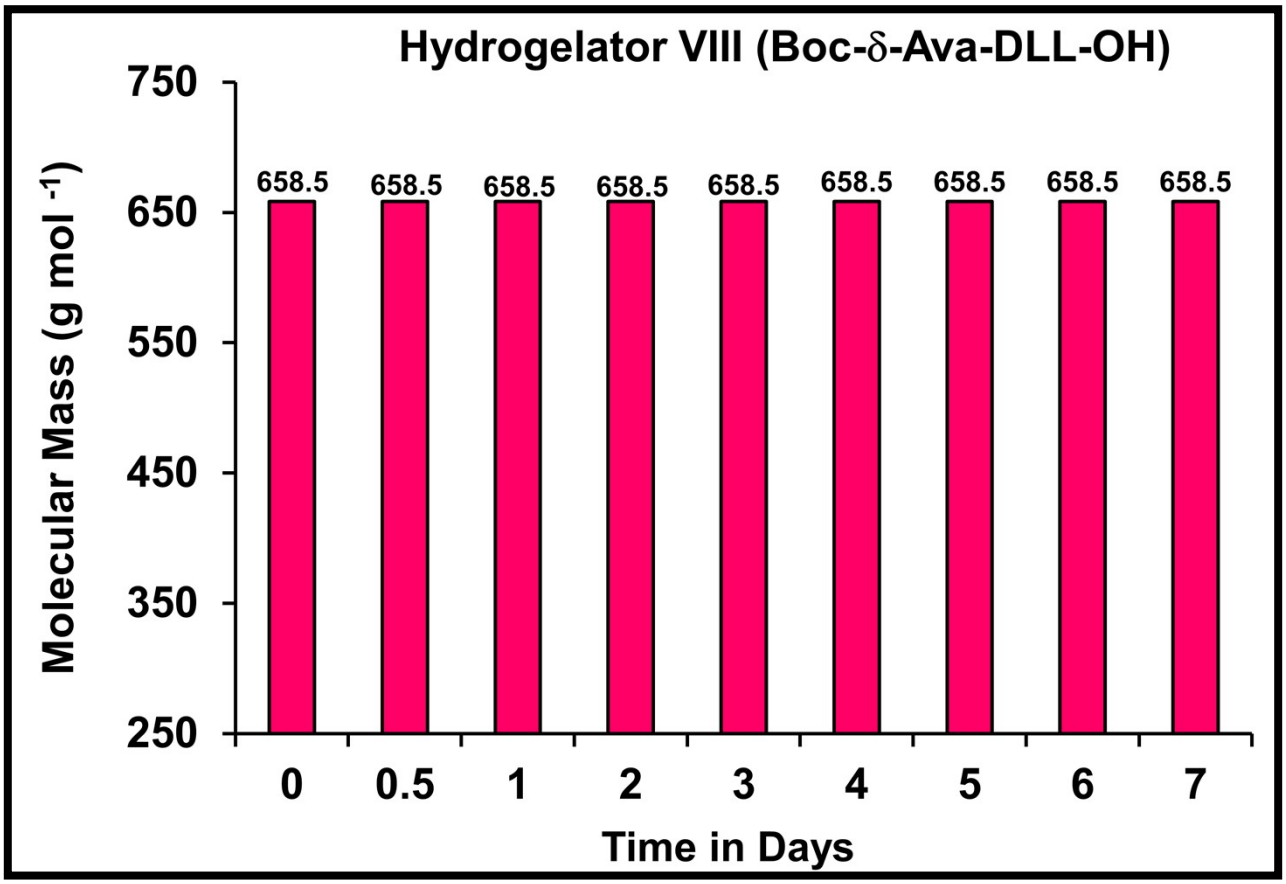

Figure S-26: - Enlarged Proteolytic Stability plot for Hydrogelator **VIII**

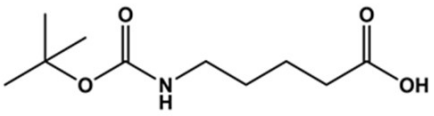

Fragment 1 : Boc-δ-Ava-OH
(217.27 m/z)

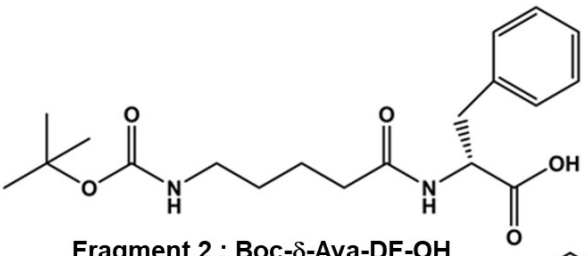

Fragment 2 : Boc-δ-Ava-DF-OH
(364.44 m/z)

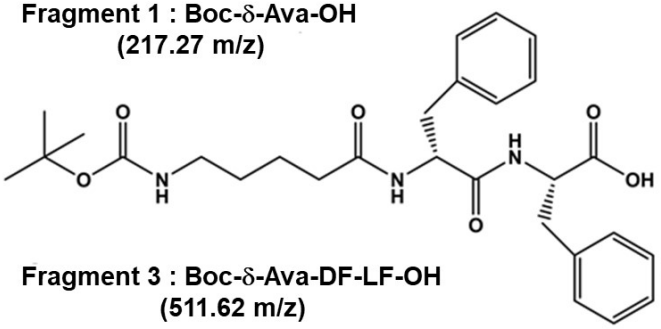

Fragment 3 : Boc-δ-Ava-DF-LF-OH
(511.62 m/z)

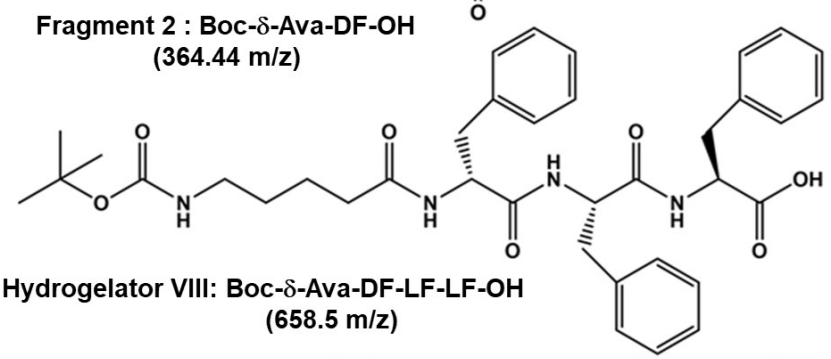

Hydrogelator VIII: Boc-δ-Ava-DF-LF-LF-OH
(658.5 m/z)

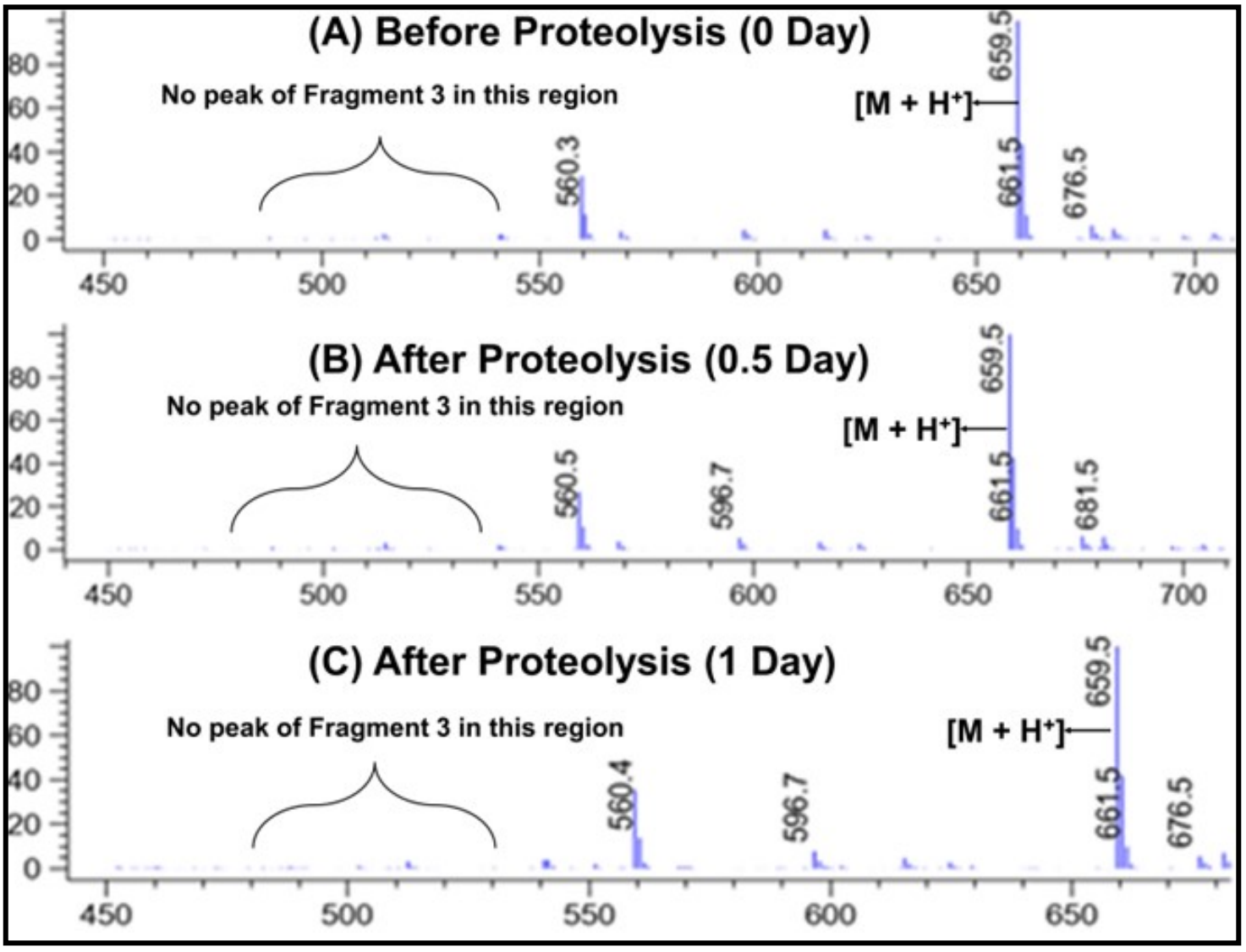

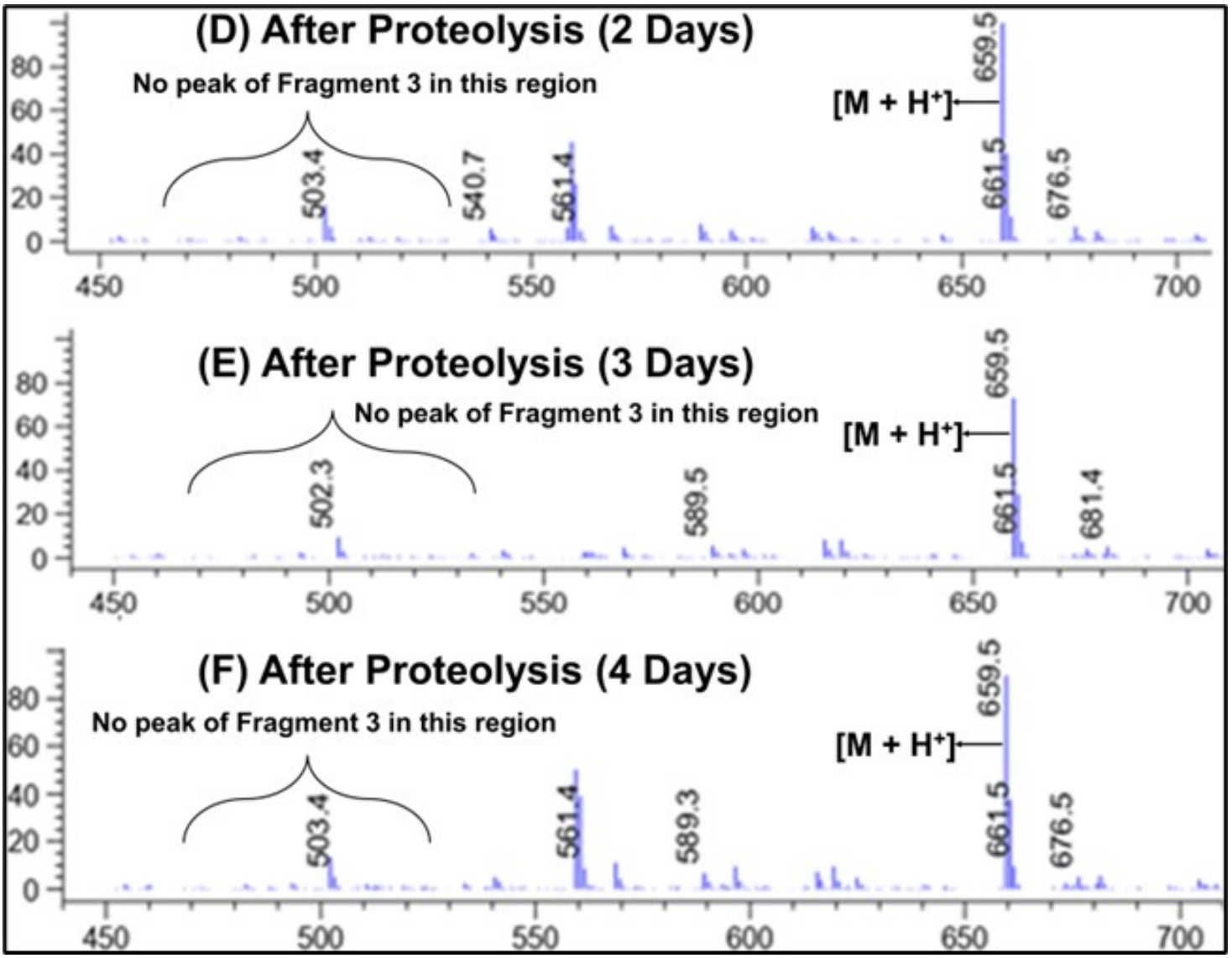
(D) After Proteolysis (2 Days)
No peak of Fragment 3 in this region
[M + H+]
503.4
540.7
561.4
659.5
661.5
676.5
(E) After Proteolysis (3 Days)
No peak of Fragment 3 in this region
[M + H+]
502.3
589.5
659.5
661.5
681.4
(F) After Proteolysis (4 Days)
No peak of Fragment 3 in this region
[M + H+]
503.4
561.4
589.3
659.5
661.5
676.5
0
20
40
60
80
450
500
550
600
650
700

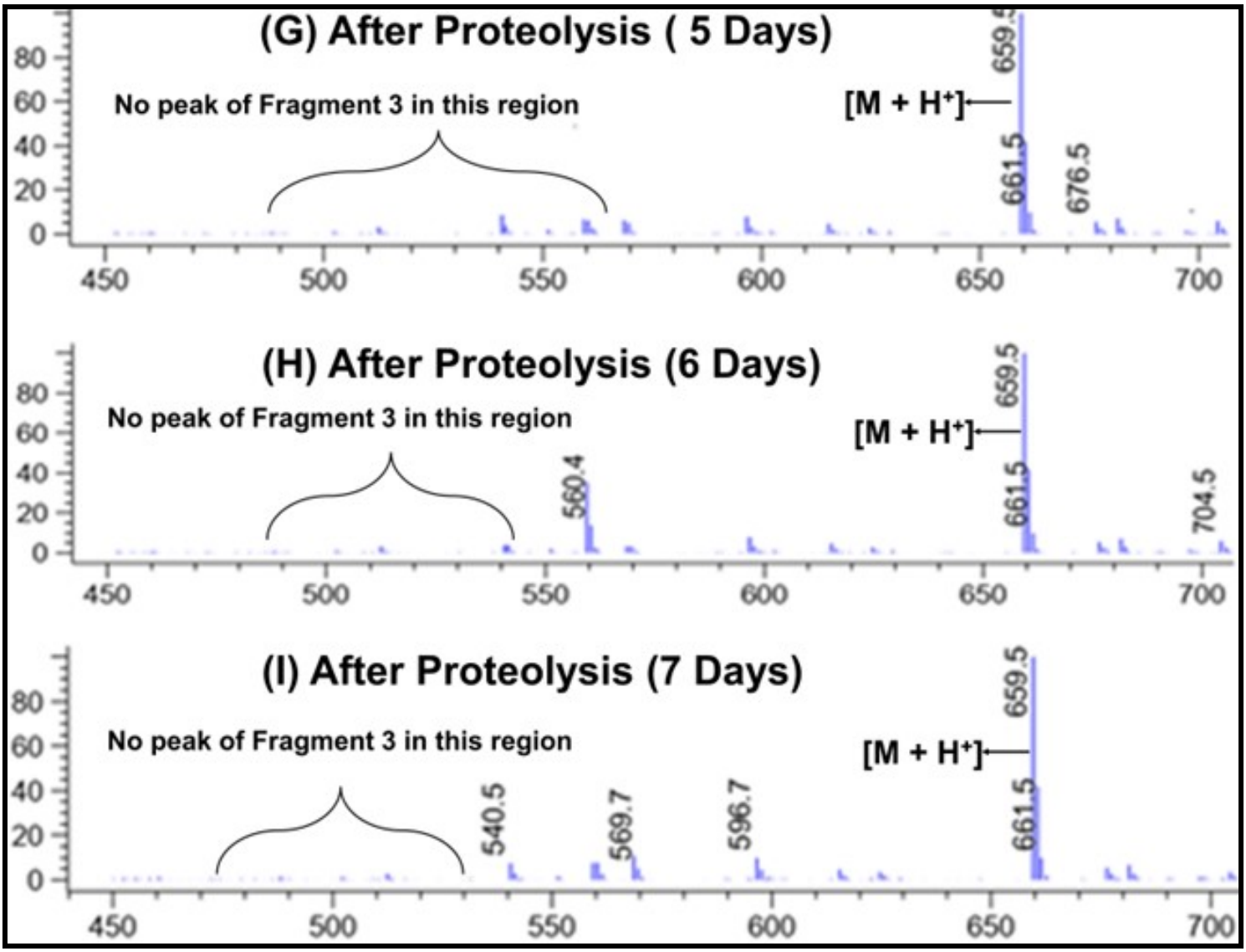

Figure S-27 (A - I): - Structures of the possible fragments that could be obtained during the proteolytic experiments(top). Mass Spectra of the Hydrogelator **VIII**, recorded at different time intervals of the Experiment (A-I).

Table – S6: - Data of MTT Assay, Hemolytic Assay and Lipid Peroxidation Assay for Hydrogelator **VIII**

MTT Assay	**NC (mM)**	**15.78 (mM)**	**31.25 (mM)**	**62.5 (mM)**	**125 (mM)**	**250 (mM)**	**500 (mM)**	**-**
DLL H-VIII	100	87.93	73.68	66.32	54.20	32.08	30.66	**-**
Hemolytic Assay	**Positive Control (µg/mL)**	**Negative Control (µg/mL)**	**6.25 (µg/mL)**	**12.5 (µg/mL)**	**25 (µg/mL)**	**50 (µg/mL)**	**100 (µg /mL)**	**200 (µg/mL)**
DLL H-VIII	**100**	**0**	**0**	**0**	2.19	12.02	29.51	40.44
Lipid Peroxidation Assay	**1.5 (mmol)**	**2.5 (mmol)**	**5 (mmol)**	**10 (mmol)**	**20 (mmol)**	**-**	**-**	**-**
DLL H-VIII	15.6	13.2	11	10.4	9.8	**-**	**-**	**-**

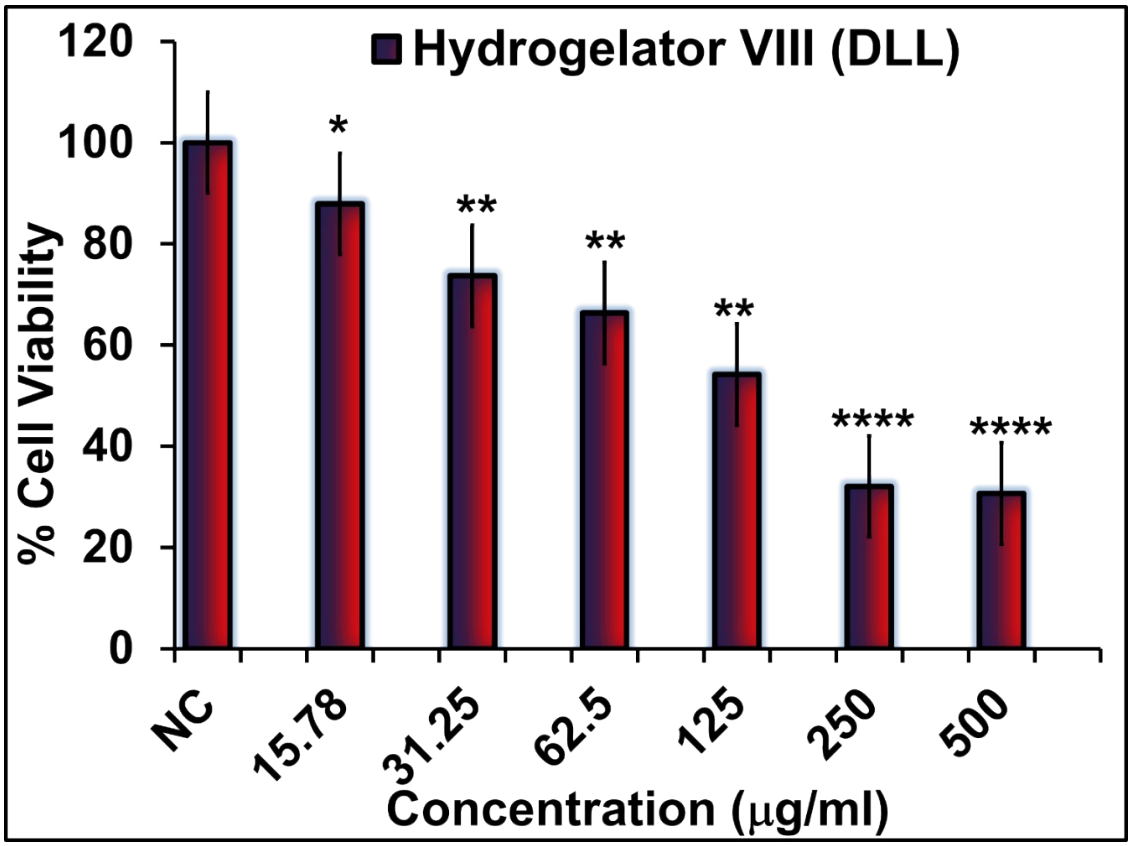

Figure S-28: - Enlarged MTT Assay for Hydrogelator **VIII.** Data was statistically analysed using a two-tailed paired Student's t test and presented as mean ± SD (N = 3). *p<0.05; **p<0.01; ****p < 0.0001, as compared to the negative control group.

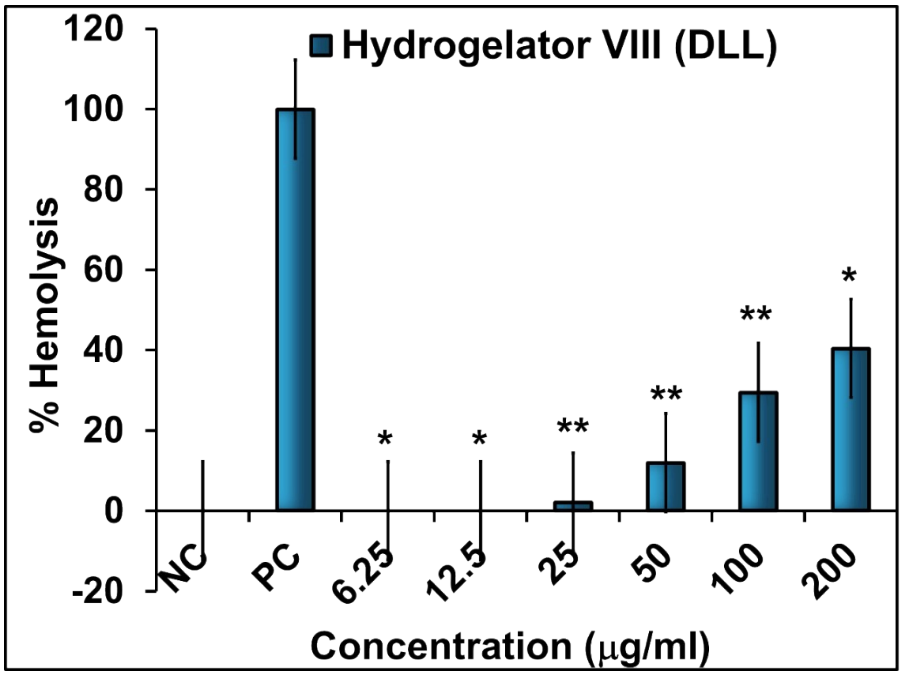

Figure S-29: - Enlarged Hemolytic Assay of Hydrogelator **VIII.** Data was statistically analysed using a two-tailed paired Student's t test and presented as mean ± SD (N = 3) *p<0.05; **p<0.01, as compared to the positive control group.

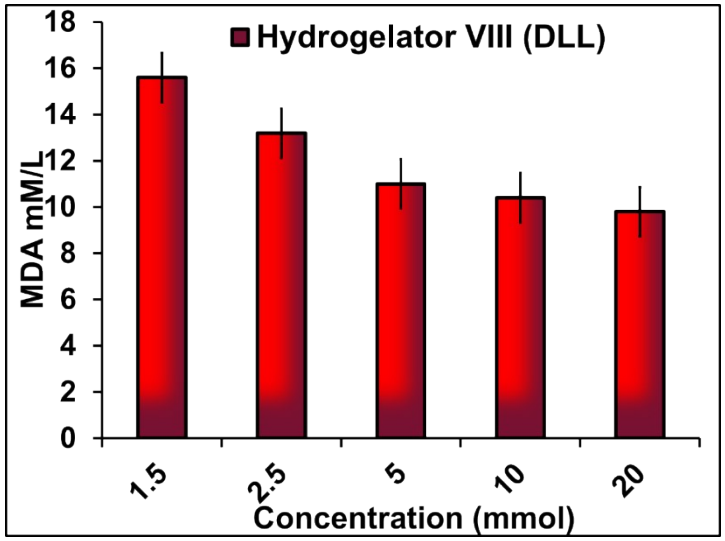

Figure S-30: - Enlarged Lipid Peroxidation Assay for Hydrogelator **VIII**

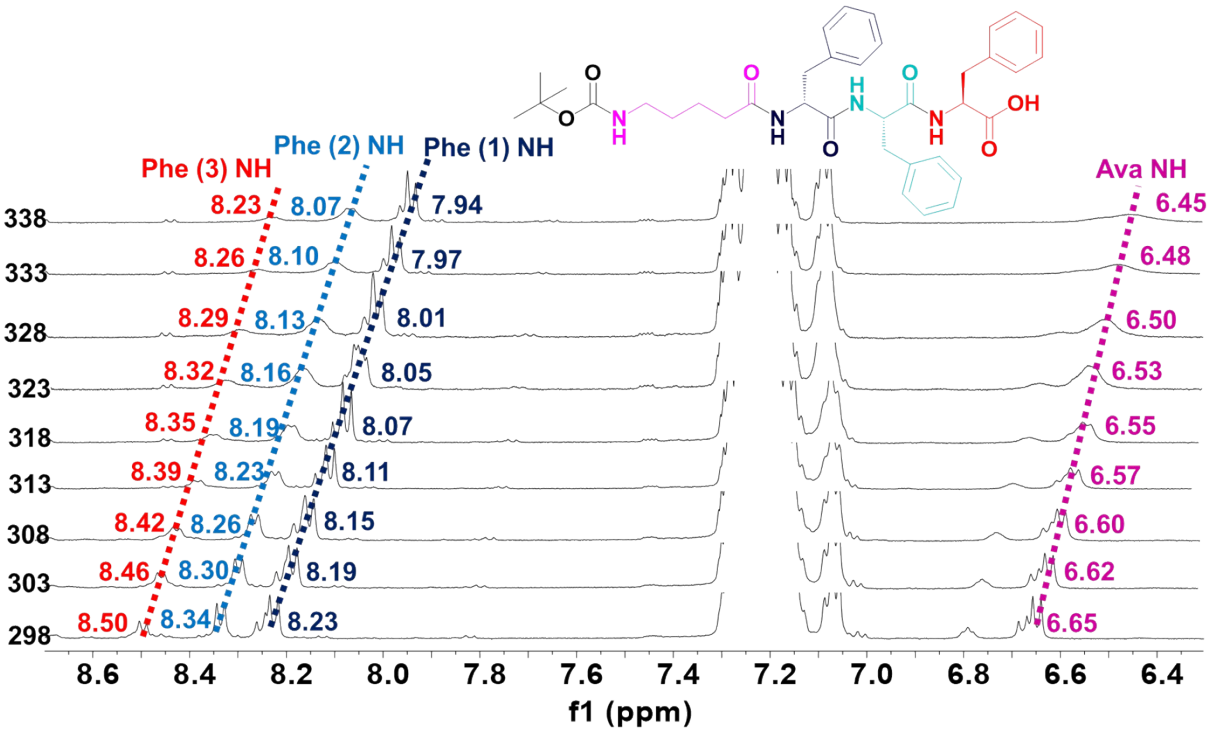

Figure S-31 (A): - Enlarged Variable Temperature Dependent NMR for Hydrogelator **VIII**

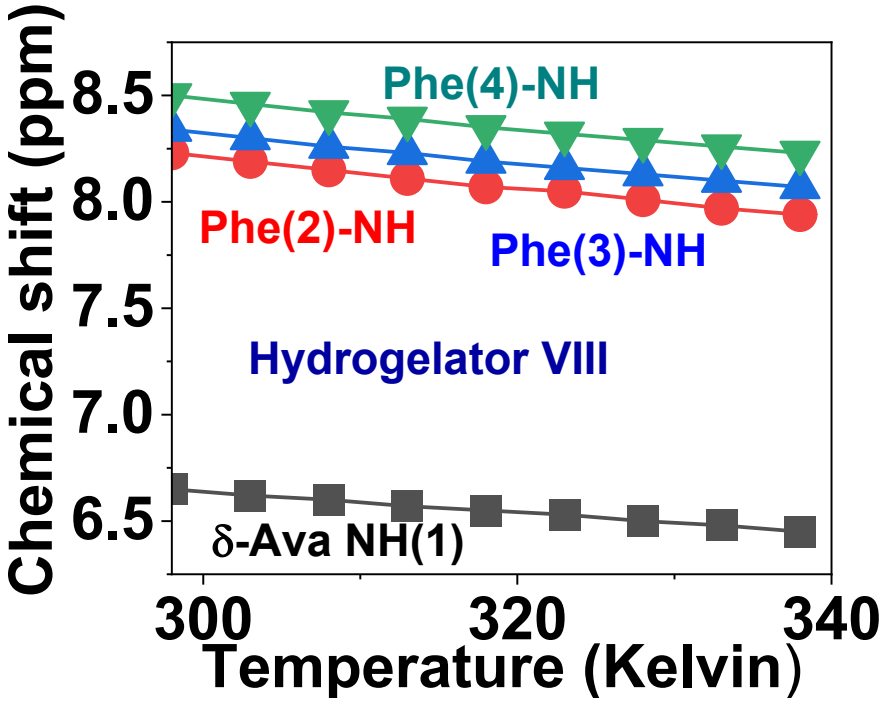

Figure S-31 (B): - Graphical representation of the variable temperature NH chemical shifts of Hydrogelator **VIII**

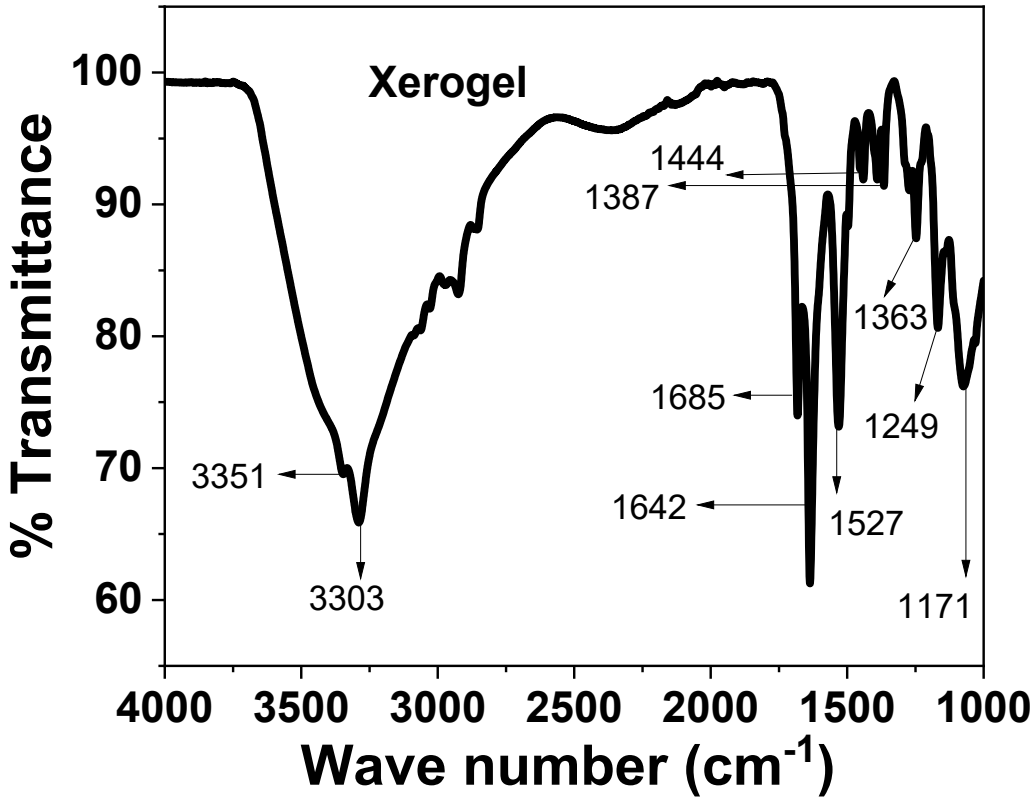

Figure S-31 (C): - Enlarged Xerogel FTIR plot for Hydrogelator **VIII**

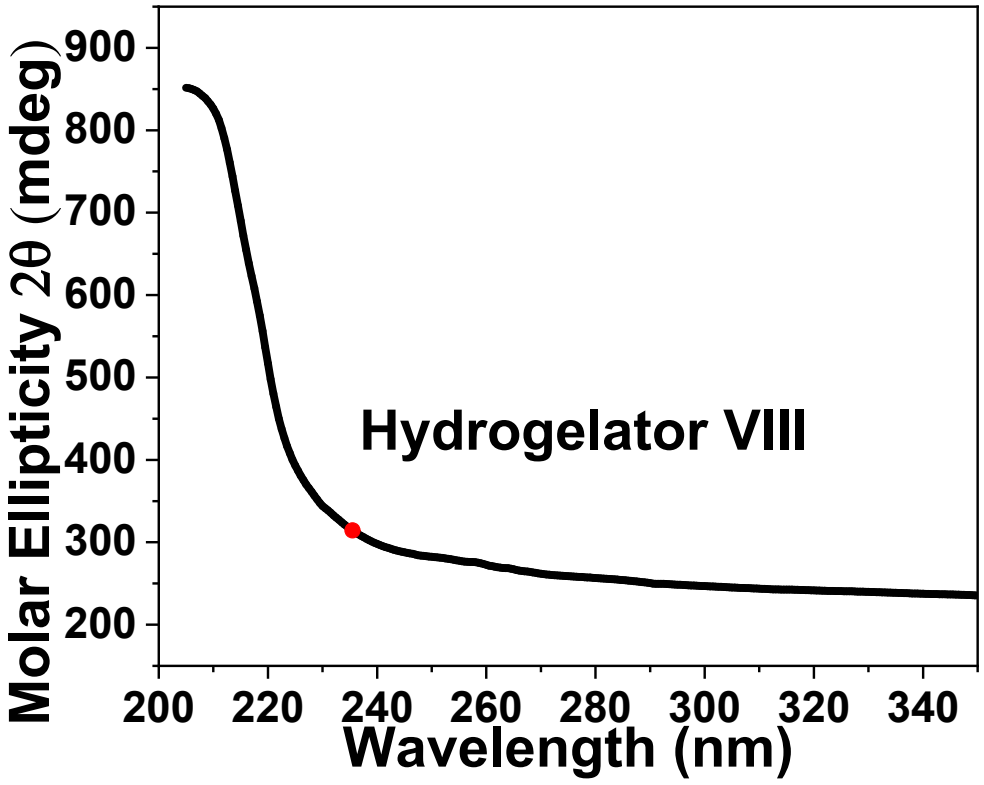

Figure S-31 (D): - Enlarged Circular Dichroism plot for Hydrogelator **VIII**

Table – S7: - *In vivo* Anti-inflammatory studies for Hydrogelator **VIII**

Hematocrit parameter	**Group 1 (Control Group)**	**Group 2 (Disease Control)**	**Group 3 (Standard Drug)**	**Group 4 (High dose)**
H.B(gm/dl)	12.3±0.570	11.8833± 0.539	12.36±0.6321	9.56± 1.5163
RBC Count (mil/cmm)	7.108±0.386	7.0033±0.137	7.146±0.3220	4.934± 0.9652
W.B.C Count (/cmm)	5250±661.68	10583.333±2441.231	5140±1915.7244	2280± 546.7581
PCV (%)	31.86±1.800	29.9833±1.029	31.16±1.9009	21.648± 3.8490
MCV (cu micron)	44.80±0.732	42.9283±1.841	44.25±1.4897	51.72± 9.2736
MCH (picograms)	17.351±0.253	17.0216±0.907	17.582±0.4101	22.65± 3.5195
MCHC (g/dl)	38.791±0.951	39.5733±0.849	39.822±0.5453	44.988± 2.0952
Neutrophils (%)	16.5±5.296	26.5±3.461	25.2±3.2110	17.2± 2.5484
Lymphocytes (%)	75.66±6.124	62.666±5.327	64±3.8013	75.6± 3.6117
Eosinophil (%)	4.166±0.542	5±0.816	5.4±0.4472	4± 0.6666
Monocytes (%)	3.5±0.619	5.333±0.988	4.4±0.6831	3.2± 0.7923
Basophils (%)	0.166±0.166	0.5±0.341	0±0	0± 0
Platelets (Lac/cmm)	8.461±0.429	7.6683±1.166	4.946±0.5097	7.012± 2.0563

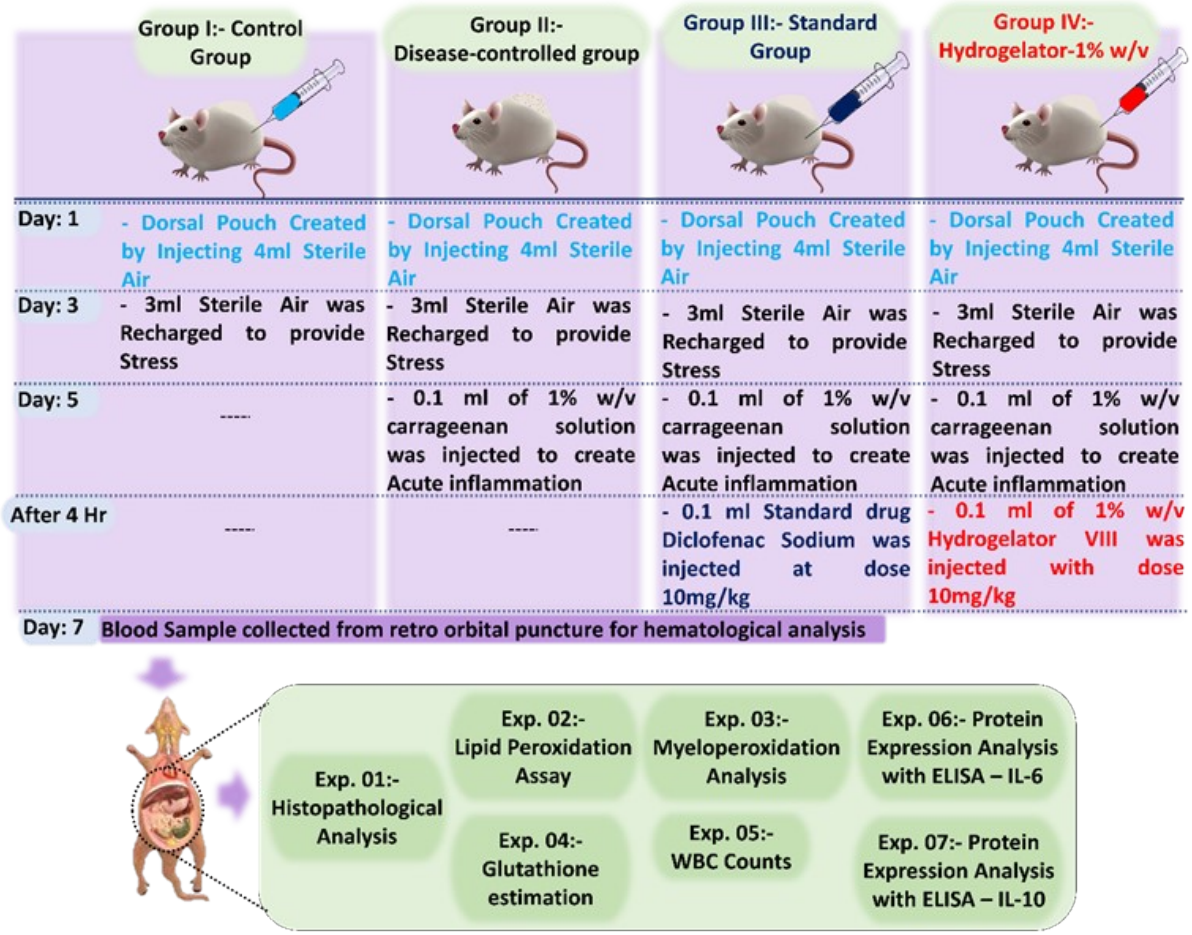

Figure S-32: Detailed protocol of the *invivo* experiments performed to prove the efficacy of Hydrogelator **VIII**. In each group there were 6 animals. The Group 1 contained Albino mice without any injury. Group 2 contained Injured animals with no drug. Group 3 contained, Injured animals treated with the marketed drug, dichlorofenac sodium . Group 4 contained albino mice treated with 1% of our designed Hydrogelator **VIII**, with all the bench Marks, embedded in them.

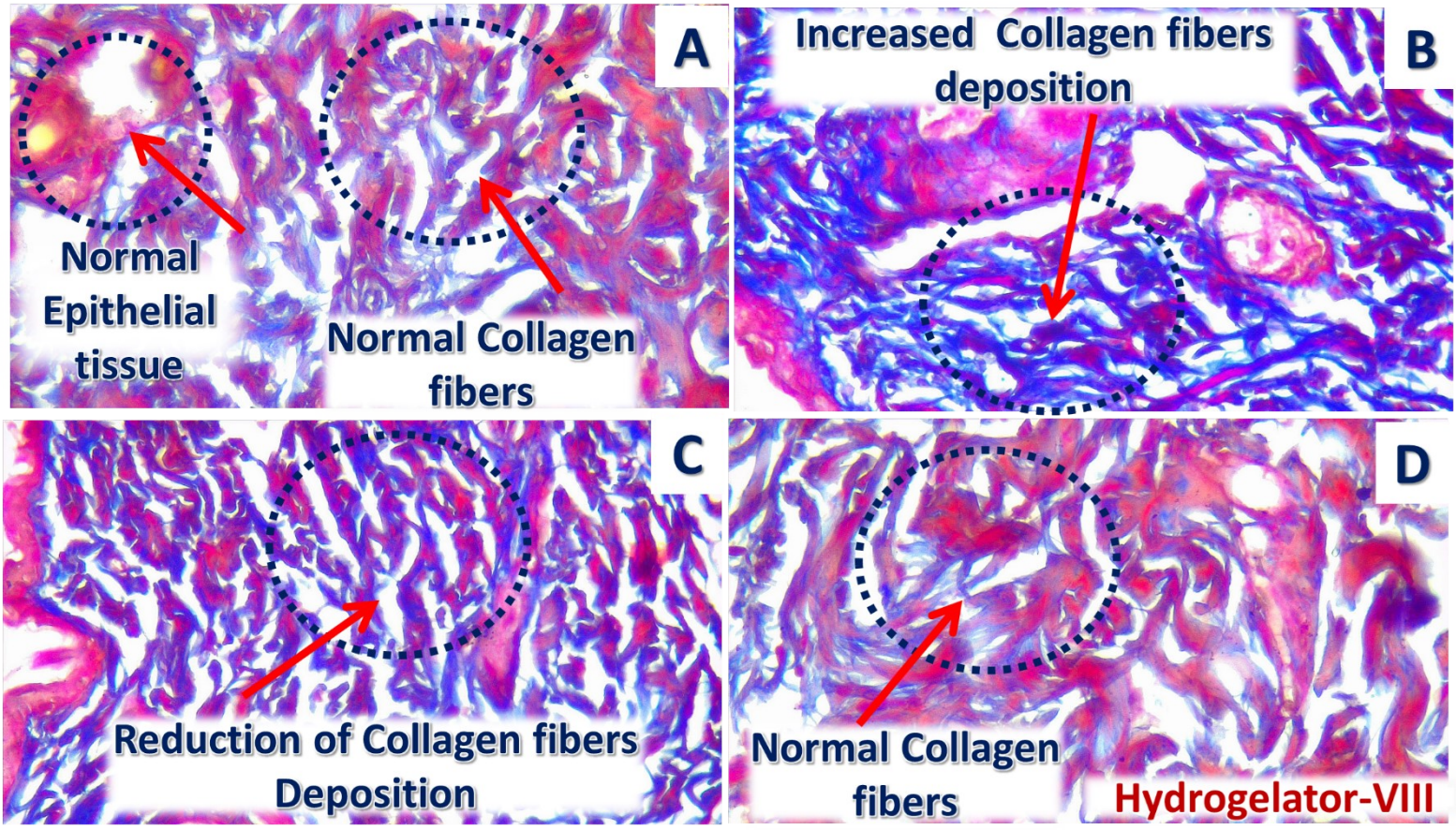

Figure S-33: Histopathological images of different groups of animals visualized by Masson Trichrome staining for collagen deposition technique and examined under 100X resolution. In this technique the collagen fibers are stained blue and healthy area red. As evident from the images of Group 1 animals, maximum red region was observed indicating normal architecture, with minimum collagen deposition **A)** ; Group 2: animals demonstrated increased collagen fibre deposition with enhanced blue units in the figure **B)** Group 3: indicated significant improvement as compared to Group 1, with reduced collagen deposition (blue) **C).**; Finally, Group 4: animals exhibited tissue architecture comparable to the normal rats with maximum red region with minimum collagen deposition (blue) comparable to the control (**D**).

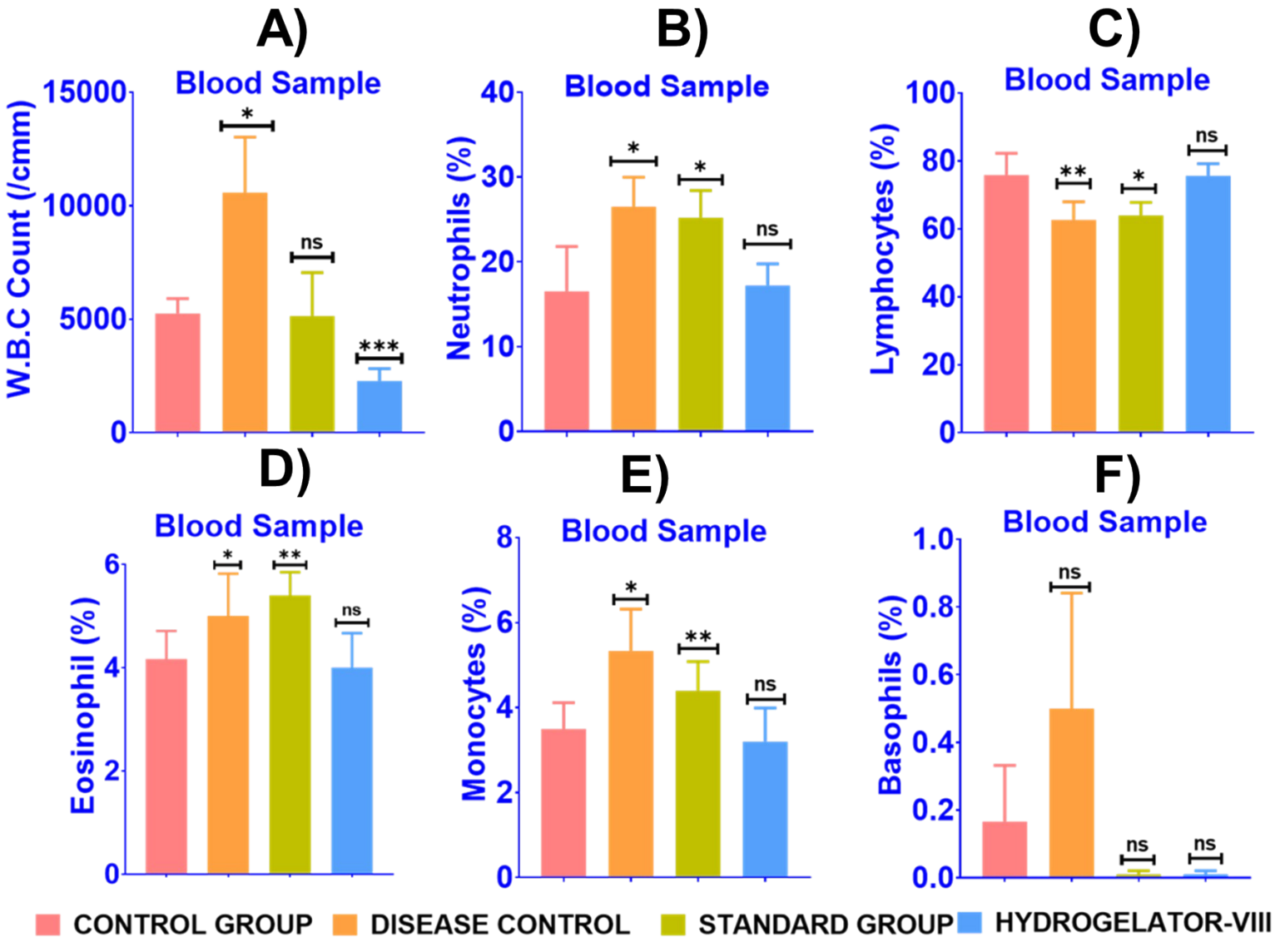

Figure S-34 (A-F): Hematocrit Study from different groups of animals involved in anti-inflammatory studies *in vivo.* Data was statistically analysed using a two-tailed paired Student's t test .(N = 6). ns = Not Significant, *p<0.05; **p<0.01, as compared to the control group.

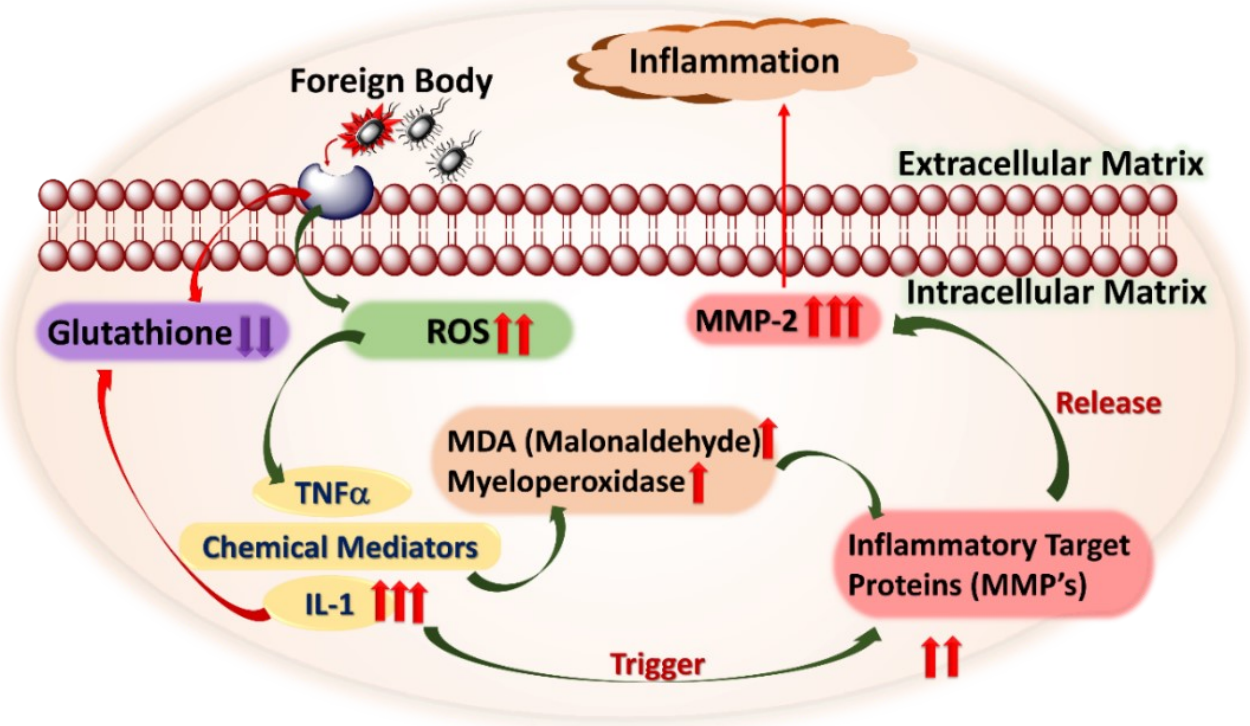

Figure S35: Probable Mechanism of Inflammation in tissues. From the literature documentation, the Inflammation process commences with the Triggering Event, where foreign substances in the form of microbial infection or others, injure the tissues causing oxidative stress. Eventually accentuation of the level of toxins takes place, leading to the accumulation of high concentrations of reactive oxygen species (ROS) in the body. Next, vascular changes occur, compelling the release of some chemical mediators that not only trigger a cluster of cytokines such as TNF-α, IL1, chemokines, and others, but also two different biomarkers malonaldehyde and myeloperoxidase. Thus collectively, they act on inflammatory target proteins, to release Matrix Metalloproteinases, one of the main culprit for inflammation. On the other hand, a different mechanism simultaneously operates involving glutathiones (GSH). Studies reveal that a reduction in GSH concentration results in enhanced levels of proinflammatory mediators that plays a central role in causing inflammatory associated diseases. As an outcome, the proportion of malonaldehyde and myloperoxidase increases. So, glutathione levels mainly decrease on one hand by the attack of the microbes and secondly by the effect of chemical mediators and biomarkers. Besides, the higher is the concentration of the MMPs produced in the body, the greater is the extent of inflammation, reflected by an enhanced level of leucocyte infiltration at the site of injury.